MCB
Journals.ASM.org

Loss of ADAM17-Mediated Tumor Necrosis Factor Alpha Signaling in Intestinal Cells Attenuates Mucosal Atrophy in a Mouse Model of Parenteral Nutrition

Yongjia Feng,[a] Yu-Hwai Tsai,[b,c*] Weidong Xiao,[a] Matthew W. Ralls,[a] Alex Stoeck,[b*] Carole L. Wilson,[d] Elaine W. Raines,[d] Daniel H. Teitelbaum,[a] Peter J. Dempsey[b,c,e]

Section of Pediatric Surgery, Department of Surgery,[a] Division of Gastroenterology, Department of Pediatrics,[b] and Department of Molecular and Integrative Physiology,[c] University of Michigan Medical School, Ann Arbor, Michigan, USA; Department of Pathology, University of Washington, Seattle, Washington, USA[d]; Division of Gastroenterology, Hepatology and Nutrition, Department of Pediatrics, University of Colorado Medical School, Aurora, Colorado, USA[e]

Total parenteral nutrition (TPN) is commonly used clinically to sustain patients; however, TPN is associated with profound mucosal atrophy, which may adversely affect clinical outcomes. Using a mouse TPN model, removing enteral nutrition leads to decreased crypt proliferation, increased intestinal epithelial cell (IEC) apoptosis and increased mucosal tumor necrosis factor alpha (TNF-α) expression that ultimately produces mucosal atrophy. Upregulation of TNF-α signaling plays a central role in mediating TPN-induced mucosal atrophy without intact epidermal growth factor receptor (EGFR) signaling. Currently, the mechanism and the tissue-specific contributions of TNF-α signaling to TPN-induced mucosal atrophy remain unclear. ADAM17 is an ectodomain sheddase that can modulate the signaling activity of several cytokine/growth factor receptor families, including the TNF-α/TNF receptor and ErbB ligand/EGFR pathways. Using TPN-treated IEC-specific ADAM17-deficient mice, the present study demonstrates that a loss of soluble TNF-α signaling from IECs attenuates TPN-induced mucosal atrophy. Importantly, this response remains dependent on the maintenance of functional EGFR signaling in IECs. TNF-α blockade in wild-type mice receiving TPN confirmed that soluble TNF-α signaling is responsible for downregulation of EGFR signaling in IECs. These results demonstrate that ADAM17-mediated TNF-α signaling from IECs has a significant role in the development of the proinflammatory state and mucosal atrophy observed in TPN-treated mice.

Although total parenteral nutrition (TPN) is an essential therapy for patients who cannot tolerate enteral nutrition, there are numerous and significant clinical sequelae associated with TPN treatment (1). These clinical complications, which include altered immunological responses, hepatic dysfunction, metabolic derangements, endotoxemia, bacterial infections, and sepsis, can delay or make it difficult to wean patients back onto enteral nutrition. Several studies have indicated that early TPN administration in critically ill patients is associated with worsened clinical outcomes and increased rates of septicemia, often from enterically derived organisms (1, 2). These issues clearly highlight that a more detailed understanding of the underlying mechanisms of TPN-related intestinal complications is needed both to improve the selection and administration of TPN to patients and for the development of new therapeutic options for patients dependent on TPN.

The mouse model of TPN represents an ideal system to study signal transduction pathways contributing to mucosal atrophy without acute inflammatory changes or intestinal epithelial cell (IEC) destruction seen in other intestinal injury/inflammation models. The removal of enteral nutrition is associated with decreased crypt proliferation, increased IEC apoptosis, a loss of epithelial barrier function (EBF), and altered enteric microbiota, resulting in a mild proinflammatory state and mucosal atrophy (1). Previous studies have shown that upregulation of tumor necrosis factor alpha (TNF-α) and its receptor (TNFR1) plays a central role in mediating TPN-induced mucosal atrophy. Importantly, epidermal growth factor receptor (EGFR) blockade studies have shown that the improved IEC responses observed in TPN-treated *TNFR1*^{KO} mice are dependent, in part, on the maintenance of functional EGFR signaling within IECs. The protective effect of EGFR signaling is further supported by the ability of exogenous EGF treatment to attenuate mucosal atrophy in TPN-treated wild-type (WT) mice (3). Detailed analysis of TPN-treated *TNFR1*^{KO}, *TNFR2*^{KO}, and *TNFR1/2*^{DKO} mice has revealed that both TNFR1 and TNFR2 signaling contribute to TPN-induced epithelial barrier dysfunction (4). In TPN-treated WT mice, the ability of TNF-α inhibitor, etanercept, to block barrier dysfunction underscores the deleterious effect of soluble TNF-α signaling in this model (4). In spite of these observations, further dissection of the tissue-specific contributions of TNF-α/TNFR signaling in the development of TPN-induced mucosal atrophy has been hin-

Received 6 February 2015 **Returned for modification** 3 March 2015
Accepted 9 July 2015

Accepted manuscript posted online 17 August 2015

Citation Feng Y, Tsai Y-H, Xiao W, Ralls MW, Stoeck A, Wilson CL, Raines EW, Teitelbaum DH, Dempsey PJ. 2015. Loss of ADAM17-mediated tumor necrosis factor alpha signaling in intestinal cells attenuates mucosal atrophy in a mouse model of parenteral nutrition. Mol Cell Biol 35:3604–3621. doi:10.1128/MCB.00143-15.

Address correspondence to Daniel H. Teitelbaum, dttlbm@med.umich.edu, or Peter J. Dempsey, peter.dempsey@ucdenver.edu.

* Present address: Yu-Hwai Tsai, Department of Internal Medicine, University of Michigan, Ann Arbor, Michigan, USA; Alex Stoeck, Merck Research Laboratories, Boston, Massachusetts, USA.

Supplemental material for this article may be found at http://dx.doi.org/10.1128/MCB.00143-15.

dered by the lack of conditional tissue-specific *TNFα/TNFR*^{KO} mice.

ADAM17 (also termed TNF-α-converting enzyme [TACE]) is a disintegrin-metalloproteinase that acts as an ectodomain sheddase to modulate signaling activity of a variety of membrane-anchored cytokines/growth factors and their receptors (5, 6). ADAM17 was originally discovered as the proteinase responsible for the ectodomain processing of membrane-anchored TNF-α (mTNF-α) to generate soluble TNF-α (sTNF-α) (7, 8). Further analysis of ADAM17-deficient (*Tace*$^{\Delta Zn/\Delta Zn}$) mice has revealed that ADAM17 is also required for the shedding of TNFR1 and TNFR2. Paradoxically, TNFR ectodomain shedding can decrease TNFR signaling by reducing functional receptor levels at the cell surface and by the subsequent generation of soluble TNFR ectodomains that can act as decoy receptors (9–11). The complex modulation of TNF-α signaling by ADAM17 is further complicated by the fact that membrane-anchored TNF-α preferentially binds to high-affinity TNFR2 rather than low-affinity TNFR1 (12). Thus, the outcome of productive TNF-α/TNFR signaling at a cellular level is highly dependent on integration of ADAM17-mediated TNF-α and TNFR shedding events.

Using *Tace*$^{\Delta Zn/\Delta Zn}$ null mice, we previously showed that non-lymphocyte expression of ADAM17 was required for normal T cell development, peripheral B cell maturation, and lymphoid organ structure formation (10, 13). The developmental loss of TNF-α signaling in *Tace*$^{\Delta Zn/\Delta Zn}$ mice was indicated by the impaired B cell follicle organization and germinal center formation in secondary lymphoid organs, including Peyer's patches, in these ADAM17-deficient mice which phenotypically overlaps with TNF-α-deficient mice (10, 12). However, the ability of ADAM17 to regulate ectodomain processing of additional substrates was clearly demonstrated by the fact that *Tace*$^{\Delta Zn/\Delta Zn}$ mice display perinatal lethality, whereas TNF-α-deficient mice or mice lacking TNFRs are viable and fertile (11, 12). The developmental defects observed in *Tace*$^{\Delta Zn/\Delta Zn}$ mice are characteristic of EGFR-deficient (*Egfr*$^{-/-}$) mice (14, 15), and the defects in skin, heart valve, and mammary gland development have been directly attributed to the inability to process and activate specific EGFR ligands (16–19).

Due to the perinatal lethality of *Tace*$^{\Delta Zn/\Delta Zn}$ mice (10, 11), a comprehensive analysis of the intestinal phenotype of ADAM17-deficient mice has not been performed. However, recent reports of pediatric patients with ADAM17 deficiency and mice expressing hypomorphic *Adam17* alleles have been described where reduced ADAM17 activity is associated with heightened inflammatory responses in the skin and intestine (20–23). Although ADAM17 deficiency did not directly alter crypt-villus architecture under normal physiological conditions, hypomorphic ADAM17 mice showed an exacerbated dextran sodium sulfate (DSS) colitis phenotype, which was linked to a loss of TLR-mediated ADAM17-dependent shedding of EGFR ligands and downstream EGFR signaling in nonhematopoietic cells (21). These results are consistent with a cytoprotective role of IEC-specific EGFR/ErbB signaling in the DSS colitis model (24–26), but the exact cellular contribution of ADAM17 signaling from IECs and other nonhematopoietic cells within lamina propria has not been defined.

Because ADAM17 plays an important role in modulation of TNFR and EGFR/ErbB signaling *in vivo*, we hypothesized that ADAM17 may be a critical regulator of TPN-mediated mucosal atrophy. However, ubiquitous expression of ADAM17 and early postnatal lethality of ADAM17-deficient mice have made it difficult to assess the role of ADAM17 signaling within the adult intestine. In the present study, we demonstrate several novel findings. First, we used a newly developed model of IEC-specific ADAM17-deficient mice to examine the effects of ADAM17 loss from IECs upon TPN-induced mucosal atrophy. Under baseline conditions, adult *IEC-ADAM17*^{KO} mice showed normal crypt-villus architecture, proliferation and intestinal function. Surprisingly, *IEC-ADAM17*^{KO} mice showed attenuated mucosal atrophy upon TPN administration with improved crypt proliferation, decreased IEC apoptosis and reduced proinflammatory cytokine expression. Mechanistically, this protective effect was due to a loss of IEC-specific TNF-α signaling and the concomitant maintenance of functional EGFR signaling in IECs. In TPN-treated WT mice, TNF-α blockade using the TNF-α inhibitor etanercept confirmed that TNF-α signaling was responsible for downregulation of EGFR signaling in IECs. We propose that ADAM17-mediated TNF-α signaling within IECs has a significant and deleterious role in the development of mucosal atrophy observed in TPN-treated mice. Beyond the findings related to TPN, the present study demonstrates several important connections between intact ADAM17 function, and the critical interrelationship between EGFR/ErbB and TNFR signaling on the gastrointestinal epithelium; this may well have implications for other inflammatory and atrophic intestinal processes.

MATERIALS AND METHODS

Mice. *Villin-Cre* and *Adam17*$^{f/f}$ mouse strains have been described previously (27–29). Intestinal epithelial cell (IEC)-specific *Adam17* deficient mice (*Villin-Cre*; *Adam17*$^{f/f}$, referred to as *IEC-Adam17*^{KO}) and genotype controls (*Adam17*$^{f/f}$) on a C57BL/6J background were used in the present study (30). Detailed description of primers used for genotyping are described elsewhere (29). Additional control animals included WT C57BL/6J mice. Mice were maintained under controlled temperature, humidity, and light conditions. All experimental procedures were conducted in accordance to the University Committee on Use and Care of Animals at the University of Michigan.

Animal model of parenteral nutrition (TPN). For the TPN model, sex- and age-matched (>10 weeks of age) mice were housed in metabolic cages to prevent coprophagia. Catheterized mice initially received 5% dextrose in 0.45 N saline, with 20 meq of KCl/liter at 4.8 ml/day as described previously (3, 31, 32). After 24 h, mice were randomized to enteral fed control or TPN groups. Enteral controls received intravenous crystalloid solution at 0.2 ml/h and standard laboratory chow. TPN mice received intravenous (i.v.) TPN solution at 4.8 ml/day. Nitrogen and energy delivery were matched between groups (isonitrogenous/isocaloric). Mice were sacrificed 7 days postcannulation using CO_2.

For EGFR kinase inhibitor studies, mice received gefitinib (2.5 mg/ml in 1% aqueous Tween 80, 200 μl; LC Laboratories, Woburn, MA) by oral gavage twice daily, starting 3 days before i.v. cannulation and continuing until mice were sacrificed (3). gefitinib is a specific inhibitor for EGFR and does not cross-react with other ErbB receptors (33). For TNF-α inhibitor studies, mice received etanercept (soluble TNFR2/Fc fusion protein, 200 μg/kg in 0.1% mannitol–phosphate-buffered saline; Amgen Corp., Thousand Oaks, CA) subcutaneously (s.c.), starting 2 days before i.v. cannulation and continuing every 48 h a total of three times, and another dose of 500 μg/kg (s.c.) was given 3 h before sacrifice (4, 34, 35). Etanercept can also neutralize the TNFR1 ligand, lymphotoxin-α (12). For both inhibitor studies, control mice received a vehicle solution. For exogenous TNF-α studies, mice were injected i.v. with recombinant mouse TNF-α (200 ng/g; ImmunoTools, Friesoythe, Germany) 3 h before sacrifice. In Ussing chamber studies, this TNF-α treatment regime leads to a physiological loss of barrier function (4, 36).

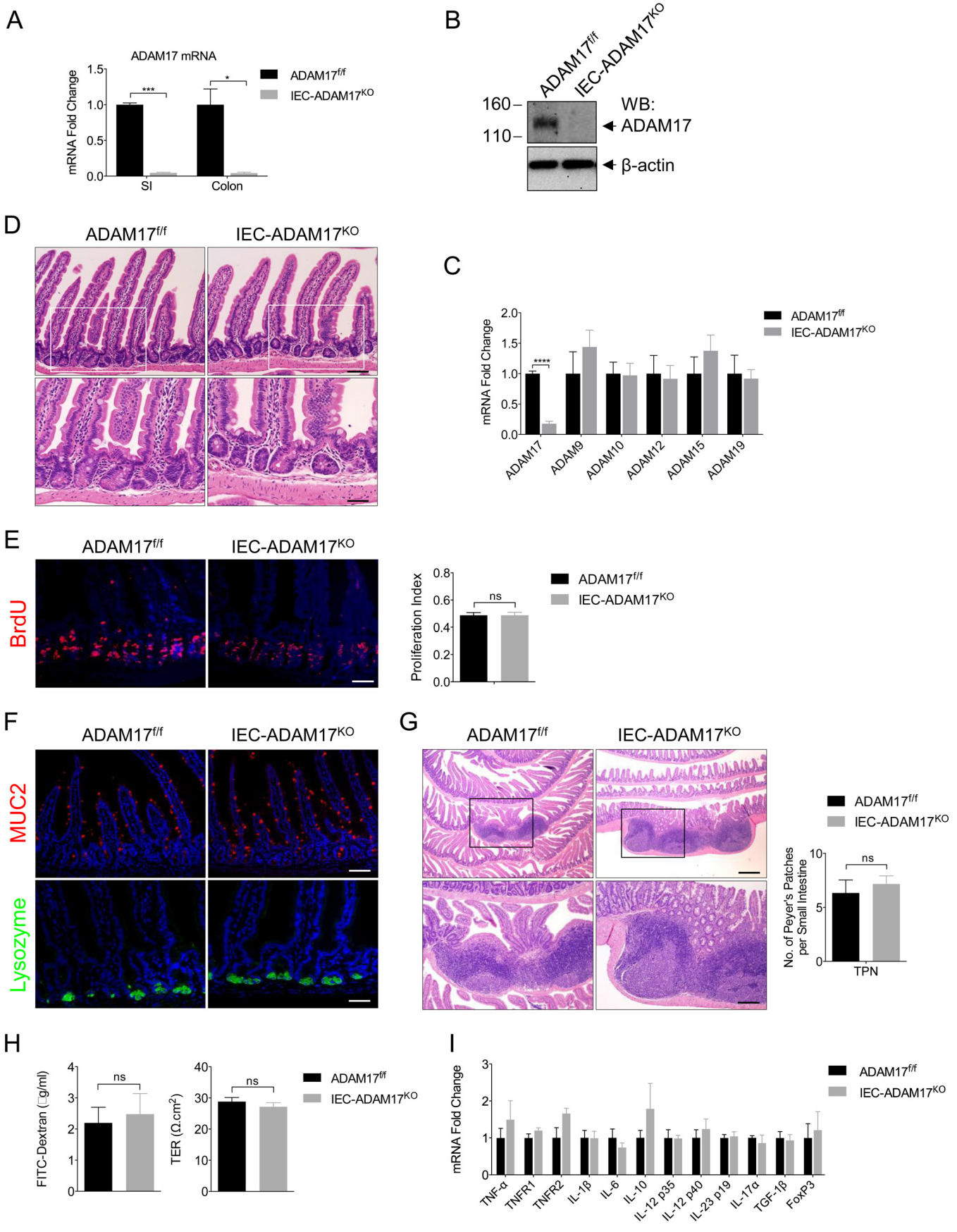
A
ADAM17 mRNA
mRNA Fold Change
1.5
1.0
0.5
0.0
***
*
SI
Colon
ADAM17f/f
IEC-ADAM17KO
B
ADAM17f/f
IEC-ADAM17KO
160–
110–
WB:
ADAM17
β-actin
C
mRNA Fold Change
2.0
1.5
1.0
0.5
0.0
****
ADAM17
ADAM9
ADAM10
ADAM12
ADAM15
ADAM19
ADAM17f/f
IEC-ADAM17KO
D
ADAM17f/f
IEC-ADAM17KO
E
ADAM17f/f
IEC-ADAM17KO
BrdU
Proliferation Index
0.8
0.6
0.4
0.2
0.0
ns
ADAM17f/f
IEC-ADAM17KO
F
ADAM17f/f
IEC-ADAM17KO
MUC2
Lysozyme
G
ADAM17f/f
IEC-ADAM17KO
No. of Peyer's Patches per Small Intestine
10
5
0
ns
TPN
ADAM17f/f
IEC-ADAM17KO
H
FITC-Dextran (g/ml)
4
3
2
1
0
ns
TER (Ω.cm2)
40
30
20
10
0
ns
ADAM17f/f
IEC-ADAM17KO
I
mRNA Fold Change
3
2
1
0
TNF-α
TNFR1
TNFR2
IL-1β
IL-6
IL-10
IL-12 p35
IL-12 p40
IL-23 p19
IL-17α
TGF-1β
FoxP3
ADAM17f/f
IEC-ADAM17KO

Cytokine measurements. Serum and small bowel mucosal cytokine levels were measured with using a multiplex protein assay (Millipore Corp., Billerica, MA) as described previously (4).

Real-time PCR analysis. RNA extraction from mucosal scrapings and real-time PCR were performed as previously described (3). Oligomers were designed using an optimization program (Premier Biosoft, Palo Alto, CA) (see Table S1 in the supplemental material). Real-time PCR data were normalized to β-actin (3).

Western blotting. Intestinal epithelial cells were isolated from the jejunum, protein extracts were prepared and immunoblotting performed as described previously (3). The results are expressed as a ratio to β-actin. Primary antibodies used were as follows: rabbit anti-ADAM17 (Millipore, Billerica, MA, and Abcam, Cambridge, MA); rabbit anti-EGFR, mouse anti-TNFR1, mouse anti-TNFR2, rabbit anti-phospho-p38, rabbit anti-p38, and rabbit anti-PCNA (Santa Cruz Biotechnology, Santa Cruz, CA); and mouse anti-phospho-Akt, mouse anti-Akt, anti-phospho-Stat3, anti-Stat3, mouse anti-phospho-MLC, and mouse anti-MLC (Cell Signaling Technology, Beverly, MA). Secondary antibody was either the corresponding horseradish peroxidase-conjugated goat anti-mouse antibody or goat anti-rabbit antibody (Santa Cruz).

Immunohistochemistry and immunofluorescence. Zinc-formalin-fixed (10%) and paraffin-embedded tissue sections and 4% paraformaldehyde-fixed frozen tissue sections of jejunum were stained using standard immunohistochemistry or immunofluorescent staining procedures as described previously (3, 37).

Intestinal morphology assessment. Small intestinal length from the pyloric sphincter to the ileocecal sphincter was measured. Villus height and crypt depth were measured in at least 10 well-oriented full-length crypt-villus units per specimen and averaged. The data were analyzed using commercially available digital image analysis software (NIS-Elements, AR 3.0).

IEC proliferation and apoptosis. For IEC proliferation, immunofluorescent staining of proliferating cell nuclear antigen (PCNA) was performed as described previously (3). The total number of proliferating cells per crypt was defined as the mean of proliferating cells in 10 crypts for each mouse. The results are expressed as number of PCNA-positive cells per crypt and then converted to percentage of controls (control values = 100%). PCNA protein levels in cell extracts were also expressed relative to controls. In addition, IEC proliferation was measured using 5-bromo-2-deoxyuridine (BrdU; 50 mg/kg intraperitoneally; Roche Diagnostic, Indianapolis, IN) given 2 h prior to sacrifice as described previously (3). An index of the crypt cell proliferation rate was calculated as the ratio of the number of crypt cells incorporating BrdU to the total number of crypt cells. Immunofluorescent staining for active caspase-3 was performed to assess IEC apoptosis as described previously (38). The results are expressed as an apoptotic index (the percentage of active caspase-3-positive cells/villi using a mean of 10 villi per mouse).

Intestinal epithelial resistance and permeability measurements. Ussing chambers were used to measure full-thickness intestinal epithelial barrier function (EBF) as previously described (4, 39, 40). Small intestine EBF was assessed using two approaches. First, EBF was measured by transepithelial resistance from full-thickness biopsy specimens. Intestinal permeability assay was further assessed using fluorescein isothiocyanate (FITC)-dextran as described previously (4). Briefly, FITC-conjugated dextran dissolved in water (molecular weight, 4,000) was administered rectally to mice at 2 mg/10 g (body weight). Whole blood was collected using heparinized microhematocrit capillary tubes via eye bleed 2 h after FITC-dextran administration. The fluorescence intensity in sera was analyzed using a plate reader. The concentration of FITC-dextran in sera was determined by comparison to the FITC-dextran standard curve.

Data analysis. Data were expressed as means ± the standard deviations. Statistical analysis was performed using a Student paired *t* test for the comparison of two means, a one-way analysis of variance (ANOVA) for multiple groups (with Tukey *post hoc* analysis) and a two-way ANOVA for categorical data. Statistical significance was defined as a P of <0.05.

RESULTS

IEC-specific ADAM17-deficient mice show no overt intestinal phenotype. To investigate the role of intestinal ADAM17 signaling in the mouse TPN model, we generated intestinal epithelial cell (IEC)-specific *Adam17*-deficient mice (termed *IEC-Adam17*^{KO} mice) (30). *IEC-Adam17*^{KO} mice were viable, exhibited efficient ADAM17 deletion from IECs, and had no compensatory changes in mRNA expression of other ADAMs (Fig. 1A to C). Importantly, *IEC-Adam17*^{KO} mice showed normal crypt-villus architecture and crypt cell proliferation (Fig. 1D and E), and no defects in secretory differentiation or the development and number of Peyer's patches were observed (Fig. 1F and G). In addition, no significant changes in small intestinal barrier function or cytokine gene signatures were detected in the intestine of *IEC-Adam17*^{KO} mice (Fig. 1H and I). Taken together, these results indicate that *IEC-Adam17*^{KO} mice display appropriate intestinal function under normal physiological conditions.

TPN-treated *IEC-Adam17*^{KO} mice are protected against mucosal atrophy and maintain IEC proliferation. Initial analysis of ADAM17 expression in WT mice treated with TPN for 7 days revealed no significant changes in ADAM17 mRNA or protein levels in the intestine (data not shown). To determine whether ADAM17 signaling was involved in IEC responses to TPN, we examined sham and TPN-treated *IEC-Adam17*^{KO} and genotype control (*Adam17*$^{f/f}$) mice. Hematoxylin-and-eosin (H&E) analysis revealed that TPN-treated control mice had mucosal atrophy with a significant reduction in crypt depth and villus height compared to their sham controls. In contrast, TPN-treated *IEC-Adam17*^{KO} mice showed substantial protection against mucosal atrophy with a significant increase in crypt depth and an overall improvement in small intestinal length, whereas villus height was unchanged (Fig. 2A to D). Periodic acid-Schiff (PAS) staining was unaltered in the small intestine of TPN-treated *IEC-Adam17*^{KO} mice, indicating that the protective effect observed in TPN-treated ADAM17-deficient mice was not due to altered secretory differentiation (Fig. 2E).

An important feature of WT mice receiving TPN is reduced crypt cell proliferation (3). To examine whether IEC-specific ADAM17 deficiency maintains IEC cell proliferation in the TPN

FIG 1 *IEC-Adam17*^{KO} mice have normal crypt-villus architecture and intestinal function. (A) Real-time PCR analysis of ADAM17 mRNA expression in scraped mucosa ($n = 2$ per genotype). (B) Western blot analysis of ADAM17 expression in isolated colonic crypts. (C) Real-time PCR analysis of ADAM mRNA expression in scraped mucosa ($n = 3$ to 5 per genotype). (D) H&E analysis. White boxes are shown at high magnifications in the lower panel. (E) BrdU immunostaining (left) and quantification of BrdU$^+$ cells per crypt (right) ($n = 5$ to 10 per group). (F) Immunostaining of goblet (MUC2) and Paneth (lysozyme) cell markers. (G, left) H&E analysis of Peyer's patches. Black boxes are shown at high magnifications in the lower panel. (Right) Quantification of Peyer's patches ($n = 6$ per group). (H) Paracellular permeability and TER measured in isolated jejunum ($n = 5$ to 7 per group) from sham experiments. (I) Real-time PCR analysis of cytokine mRNA expression in scraped mucosa ($n = 3$ to 5 per genotype). ns, not significant. Scale bars: panels D (bottom), E, and F (bottom), 25 μm; panels D (top) and F (top), 50 μm; panel G (top), 250 μm; panel G (bottom), 100 μm. *, $P < 0.05$; **, $P < 0.01$; ***, $P < 0.001$; ****, $P < 0.0001$; ns, not significant.

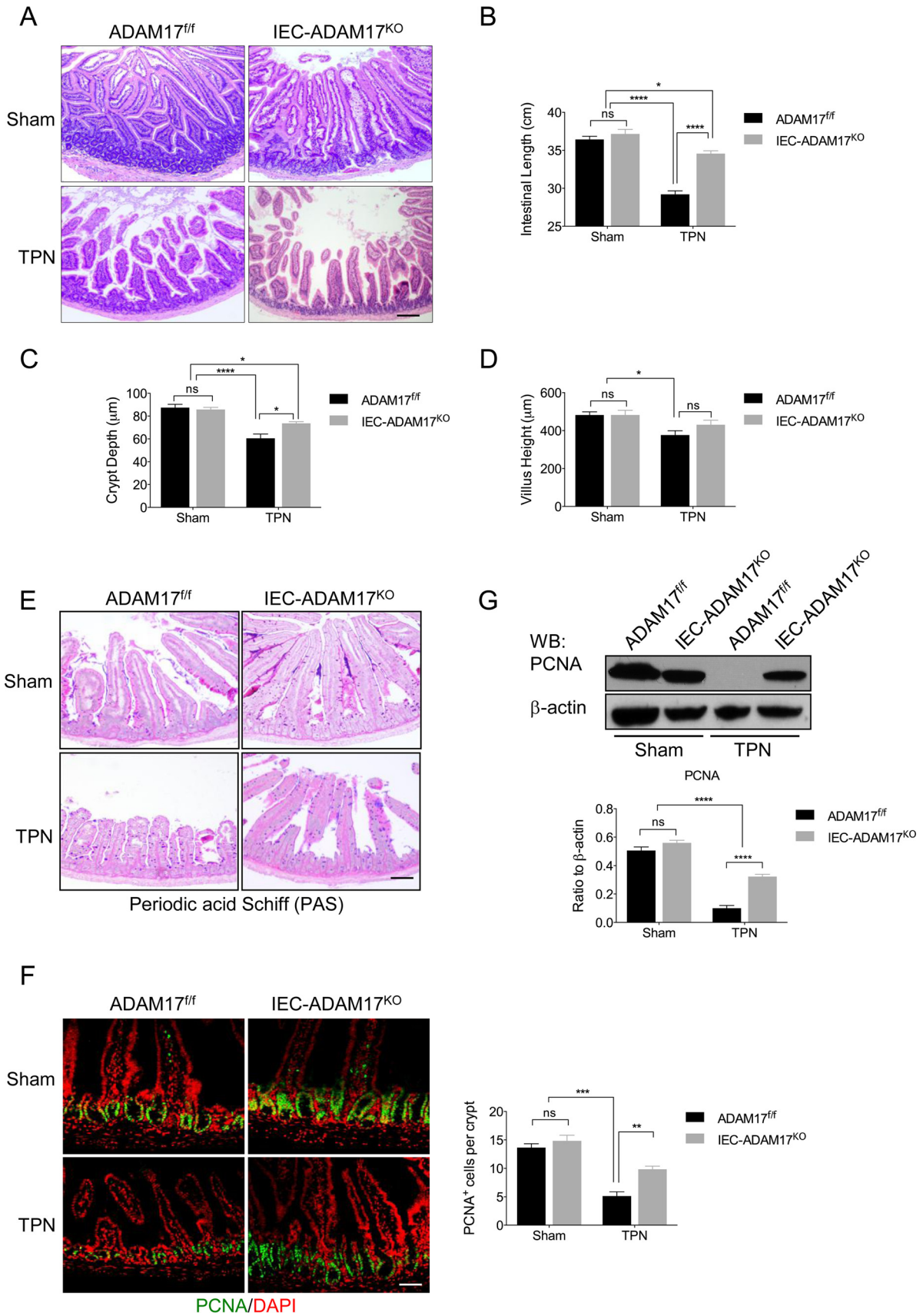

FIG 2 ADAM17 loss ameliorates the effects of TPN on mucosal atrophy and IEC proliferation. (A) H&E analysis. (B to D) Quantification of small intestinal length, crypt depth, and villus height ($n = 6$ to 8 per group). (E) Periodic acid-Schiff (PAS) staining. (F, left) Immunofluorescent staining for the cell proliferation marker, PCNA. (Right) Quantification of $PCNA^+$ cells per crypt ($n = 6$ or 7 per group). (G, top) Western blot analysis of PCNA in isolated IECs. (Bottom) Quantification of PCNA protein levels ($n = 3$ to 6 per group). *, $P < 0.05$; **, $P < 0.01$; ***, $P < 0.001$; ****, $P < 0.0001$; ns, not significant. Scale bars: panel A, 100 μm; panels E and F, 50 μm.

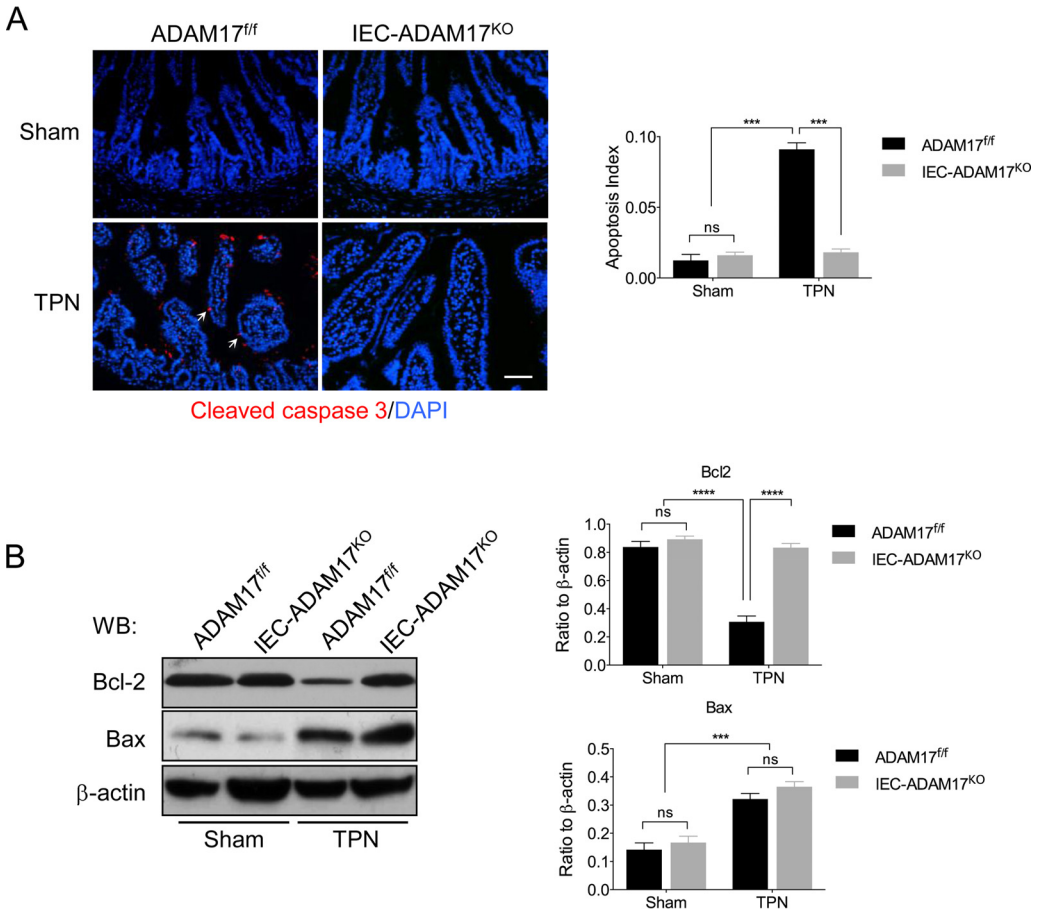

FIG 3 Reduced IEC apoptosis is observed in *IEC-Adam17*^{KO} mice receiving TPN. (A, left) Immunostaining of active caspase-3. Arrows indicate caspase-3 staining. (Right) Quantification of apoptotic index ($n = 3$ or 4 per group). Scale bar, 50 μm. (B, left) Western blot analysis of Bcl-2 and Bax in isolated IECs ($n =$ 4 or 5 per group). (Right) Quantification of Bcl2 and Bax protein levels. ***, $P < 0.001$; ****, $P < 0.0001$; ns, not significant.

model, we compared PCNA expression in both TPN-treated *IEC-Adam17*^{KO} mice and genotype controls. In agreement with previous findings, TPN-treated WT mice showed a marked reduction in PCNA staining (Fig. 2F). In contrast, TPN-treated *IEC-Adam17*^{KO} mice displayed a 2-fold increase in the number of PCNA^{+} cells in crypts compared to TPN-treated control mice (Fig. 2F). Western blot analysis of PCNA expression confirmed the retention of PCNA expression in TPN-treated ADAM17-deficient mice; although similar to the numbers of PCNA^{+} cells per crypt, the PCNA protein levels did not return completely to sham levels (Fig. 2G). Taken together, these results indicate that loss of ADAM17 signaling within IECs had a significant protective effect against TPN-induced mucosal atrophy that was associated with increased crypt height and proliferation and improved intestinal length.

TPN-treated IEC-ADAM17^{KO} mice have reduced IEC apoptosis. Enhanced IEC apoptosis is also associated with TPN-induced mucosal atrophy and is correlated with decreased Bcl-2 and increased Bax protein levels (3). To test whether the beneficial effects of intestinal ADAM17 deficiency in the TPN model extended to attenuation of IEC apoptosis, we examined activated caspase-3 expression in IECs. In TPN-treated WT control mice, a marked increase in active caspase-3 staining was observed compared to sham controls. In contrast, TPN-treated *IEC-Adam17*^{KO} mice showed a dramatic reduction in cleaved caspase-3 staining and apoptotic index with levels similar to sham controls (Fig. 3A). To determine whether the observed reduction in apoptosis correlated with changes in apoptotic regulatory proteins, Bcl-2 and Bax protein levels were measured in IECs. In TPN-treated *IEC-Adam17*^{KO} mice, Western blot analysis revealed that Bcl-2 expression was restored to sham control levels, whereas Bax levels remained elevated in both TPN-treated genotypes (Fig. 3B). Importantly, and unlike the partial restoration of cell proliferation, these results demonstrate that the protective effects observed in TPN-treated *IEC-Adam17*^{KO} mice are accompanied by retention of Bcl-2 expression and a marked reduction in IEC apoptosis.

TPN-treated *IEC-Adam17*^{KO} mice show reduced levels of soluble TNF-α signaling. Reduction of mucosal atrophy in TPN-treated *TNFR1*^{KO} mice clearly illustrates that TNFR1 signaling has important and detrimental effects on IEC responses in the TPN model (3). Because ADAM17 is the essential sheddase responsible for generating soluble TNF-α (sTNF-α), we hypothesized that the protective effect observed in TPN-treated *IEC-Adam17*^{KO} mice was to reduce sTNF-α signaling. To determine whether IEC-specific ADAM17 deletion altered TNF-α signaling, we examined the expression of TNF-α and its receptors, TNFR1 and TNFR2, in sham- and TPN-treated *IEC-Adam17*^{KO} and WT control mice. In

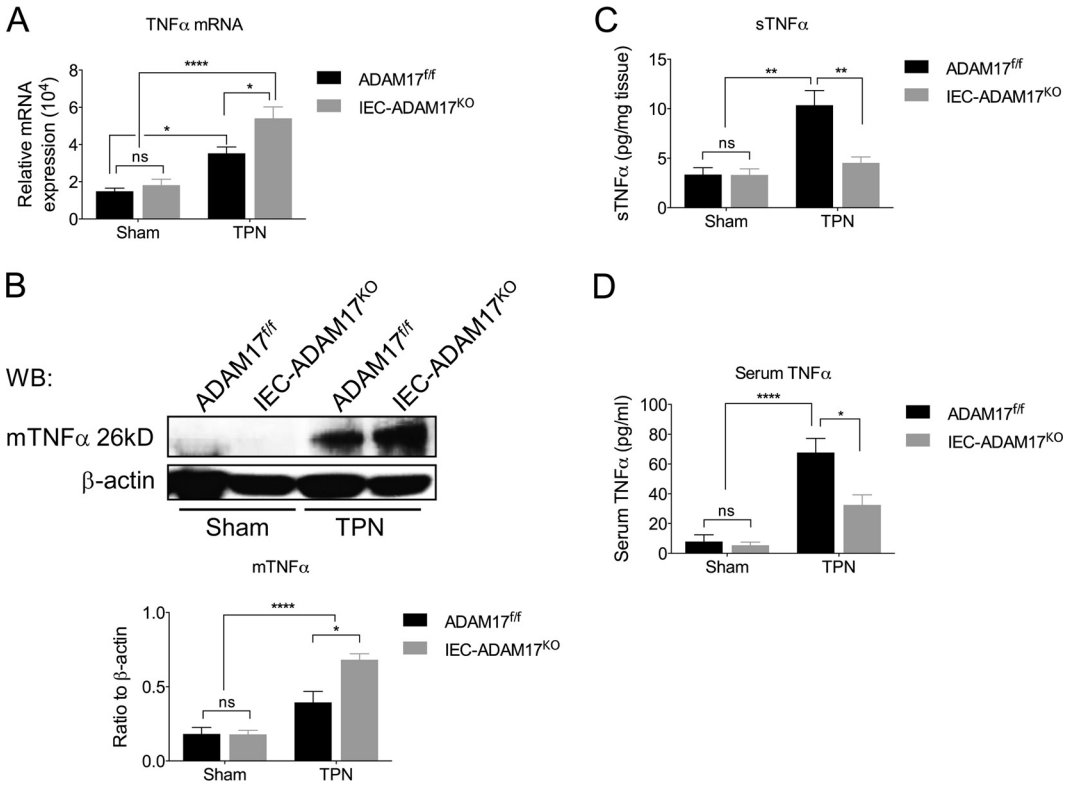

FIG 4 Soluble TNF-α levels are reduced in TPN-treated *IEC-Adam17*^{KO} mice. (A) Real-time PCR analysis of TNF-α mRNA expression in scraped mucosa (n = 4 to 6 per group). (B, top) Western blot analysis of mTNF-α in isolated IECs. (Bottom) Quantification of mTNF-α protein levels (n = 4 or 5 per group). (C and D) Quantification of sTNF-α protein levels in mucosal extracts and serum, respectively (n = 5 to 8 per group). *, $P < 0.05$; **, $P < 0.01$; ****, $P < 0.0001$; ns, not significant.

TPN-treated WT mice, both TNF-α mRNA and membrane-anchored TNF-α (mTNF-α) protein levels increased compared to sham controls (Fig. 4A and B). In addition, there was a concomitant increase in sTNF-α protein levels in both mucosal extracts and serum (Fig. 4C and D). Interestingly, TNF-α mRNA and mTNF-α protein levels were further elevated in *IEC-Adam17*^{KO} mice upon TPN administration (Fig. 4A and B). However, unlike the TPN-treated WT control mice, there was a significant decrease in sTNF protein levels in both mucosal extracts and serum of TPN-treated *IEC-Adam17*^{KO} mice (Fig. 4C and D). These results indicate that ADAM17 deficiency in IECs leads to a reduction in sTNF-α levels in TPN-treated *IEC-Adam17*^{KO} mice.

ADAM17 is also required for TNFR1 and TNFR2 shedding and modulation of cell surface TNFR populations can impact productive TNF-α signaling (9). We have previously shown that TNFR1 mRNA and protein levels are increased, whereas TNFR2 expression is unchanged in TPN-treated WT control mice (3). Although the TNFR mRNA levels in TPN-treated *IEC-Adam17*^{KO} mice were similar to TPN-treated control mice (Fig. 5A), the protein levels for both TNFR1 and TNFR2 were significantly elevated in ADAM17-deficient IECs (Fig. 5B). This result is consistent with the loss of TNFR shedding and the accumulation of cell surface TNFRs in the ADAM17-deficient state. Upon TPN administration to WT mice, we have previously shown that TNFR1 signaling increases phosphorylation of p38 mitogen-activated protein kinase (MAPK) in IECs (Fig. 5C) (3). To determine whether the findings of reduced sTNF-α protein levels and increased TNFR expression observed in TPN-treated *IEC-Adam17*^{KO} mice altered TNF-α signaling, we examined the phosphorylation status of p38 MAPK. In contrast to elevated p-p38 MAPK levels in TPN-treated WT mice, there is a partial but significant reduction in p-p38 MAPK levels in IECs from TPN-treated *IEC-Adam17*^{KO} mice (Fig. 5C). Taken together, these findings demonstrate that TPN-treated *IEC-Adam17*^{KO} mice, despite having increased TNFR1/2 protein expression, have decreased sTNF-α protein levels that results in reduced sTNF-α signaling associated with decreased p-p38 MAPK levels in IECs.

Barrier dysfunction is not attenuated in TPN-treated *IEC-Adam17*^{KO} mice but is further impaired with exogenous TNF-α. TNF-α signaling is involved in TPN-associated epithelial barrier dysfunction, and both TNFR1 and TNFR2 contribute to EBF loss (4). To determine whether IEC-specific ADAM17 deficiency improved EBF in mice receiving TPN, we measured paracellular permeability, transepithelial resistance (TER), and phosphorylation of myosin light chain (p-MLC) in IECs from sham and TPN-treated *IEC-Adam17*^{KO} and control mice. Surprisingly, despite decreased TNFR-dependent p-p38 MAPK signaling, no significant differences in EBF were observed between *IEC-Adam17*^{KO} and control mice under sham or TPN conditions (Fig. 6A to C). One possible explanation for the lack of EBF improvement in TPN-treated *IEC-Adam17*^{KO} mice is related to increased cell surface TNFR2 expression, which may differentially alter TNF-α sensitivity of ADAM17-deficient IECs. Indeed, when the above-described experiment was performed in the presence of exogenous

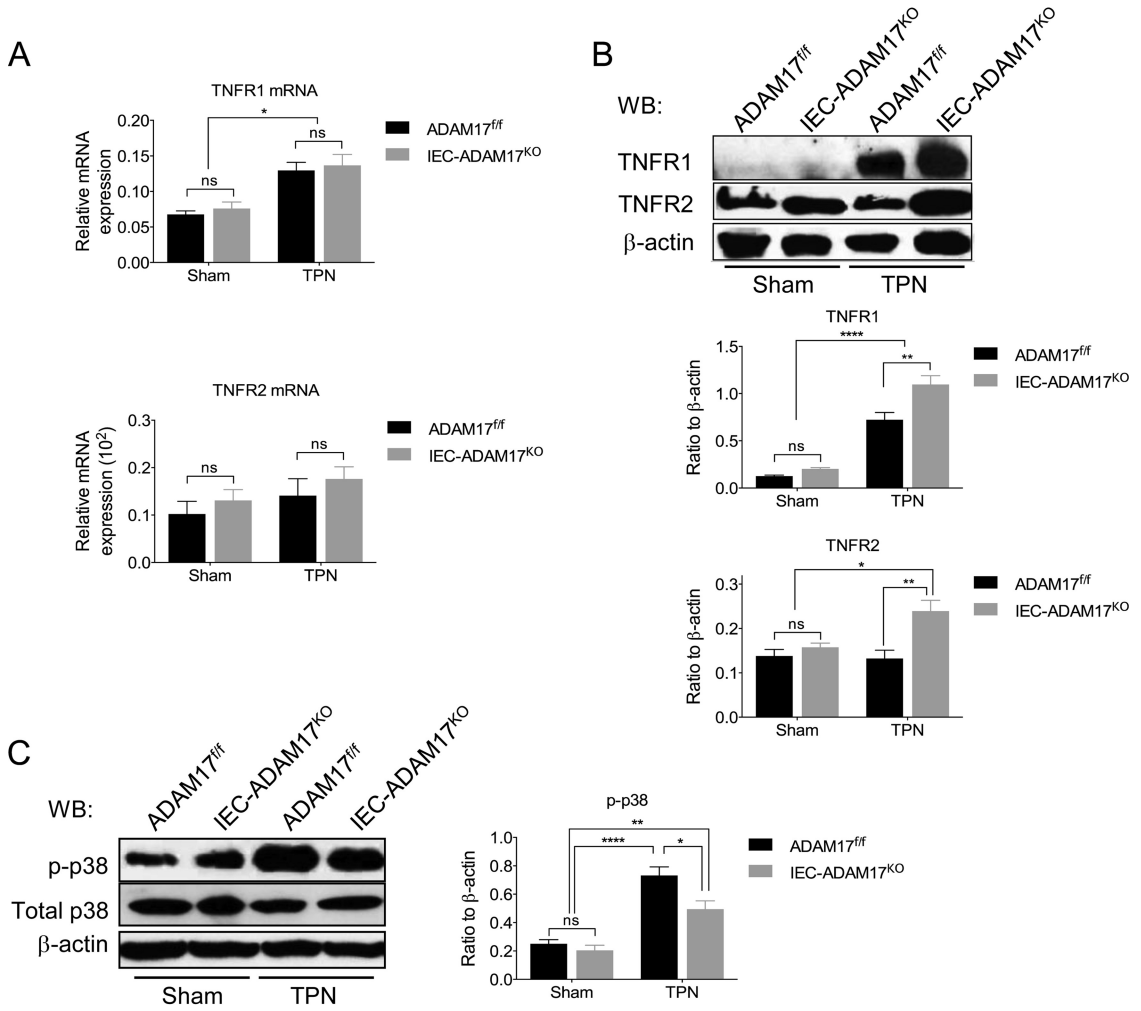

FIG 5 TNF-α signaling is reduced in IECs from TPN-treated *IEC-Adam17*^{KO} mice. (A) Real-time PCR analysis of TNFR1 and TNFR2 mRNA expression in scraped mucosa ($n = 4$ to 6 per group). (B, top) Western blot analysis of TNFR1 and TNFR2 in isolated IECs. (Middle and bottom) Quantification of TNFR1 and TNFR2 protein levels ($n = 5$ to 7 per group). (C, left) Western blot analysis of p-p38 MAPK and total p38-MAPK in isolated IECs. (Right) Quantification of p-p38 MAPK protein levels ($n = 4$ to 7 per group).*, $P < 0.05$; **, $P < 0.01$; ****, $P < 0.0001$; ns, not significant.

TNF-α a significant increase in both p-MLC levels and paracellular permeability (Fig. 6D and E) and a further but modest decrease in TER (Fig. 6F) were observed in TNF-α-treated *IEC*-Adam17^{KO} mice compared to respective TNF-α-treated genotype control groups. The effects of ADAM17 deficiency on functional TNF-α signaling in IECs are therefore complex and additional studies will be needed to dissect out the individual contributions of TNFR1 and TNFR2 signaling in this response.

Upregulation of proinflammatory cytokines is prevented in TPN-treated *IEC-Adam17*^{KO} mice. In addition to TNF-α, other proinflammatory cytokines, including interferon gamma (IFN-γ), have been implicated in mucosal atrophy and barrier dysfunction in the TPN model (39–42). To determine whether the expression of other cytokines was altered in TPN-treated *IEC-Adam17*^{KO} mice, we examined the mRNA and protein levels of several other proinflammatory cytokines from sham- and TPN-treated WT control and *IEC-Adam17*^{KO} mice. Consistent with the mild proinflammatory state produced by TPN in WT mice, the protein levels of several cytokines including IFN-γ, interleukin-6 (IL-6), IL-13, and monocyte chemotactic protein 1 (MCP-1) were significantly elevated in mucosal extracts of TPN-treated WT mice compared to sham controls (Fig. 7). In addition, both IFN-γ and IL-6 mRNA levels were markedly increased, whereas mRNA levels for all other cytokines only showed a trend toward being elevated in TPN-treated WT mice (data not shown). As expected, *IEC-Adam17*^{KO} mice expressed similar cytokine levels to WT control mice under sham conditions. However, in TPN-treated *IEC-Adam17*^{KO} mice cytokine protein levels in mucosal extracts were significantly decreased and approached sham levels (Fig. 7). Interestingly, no significant changes in cytokine mRNA and serum levels were observed except for serum IL-6 levels which were significantly elevated in TPN-treated *IEC-Adam17*^{KO} mice compared TPN-treated genotype controls (data not shown). In experimental colitis and colitis-associated cancer models, IL-6 and TNF-α can promote IEC protection and tumor promotion through cross-regulation (43). Further studies will be needed to determine whether changes in expression of IL-6 and other cytokines contribute to the attenuation of mucosal atrophy observed in TPN-treated *IEC-Adam17*^{KO} mice. However, because immune cells primarily produce these cyto-

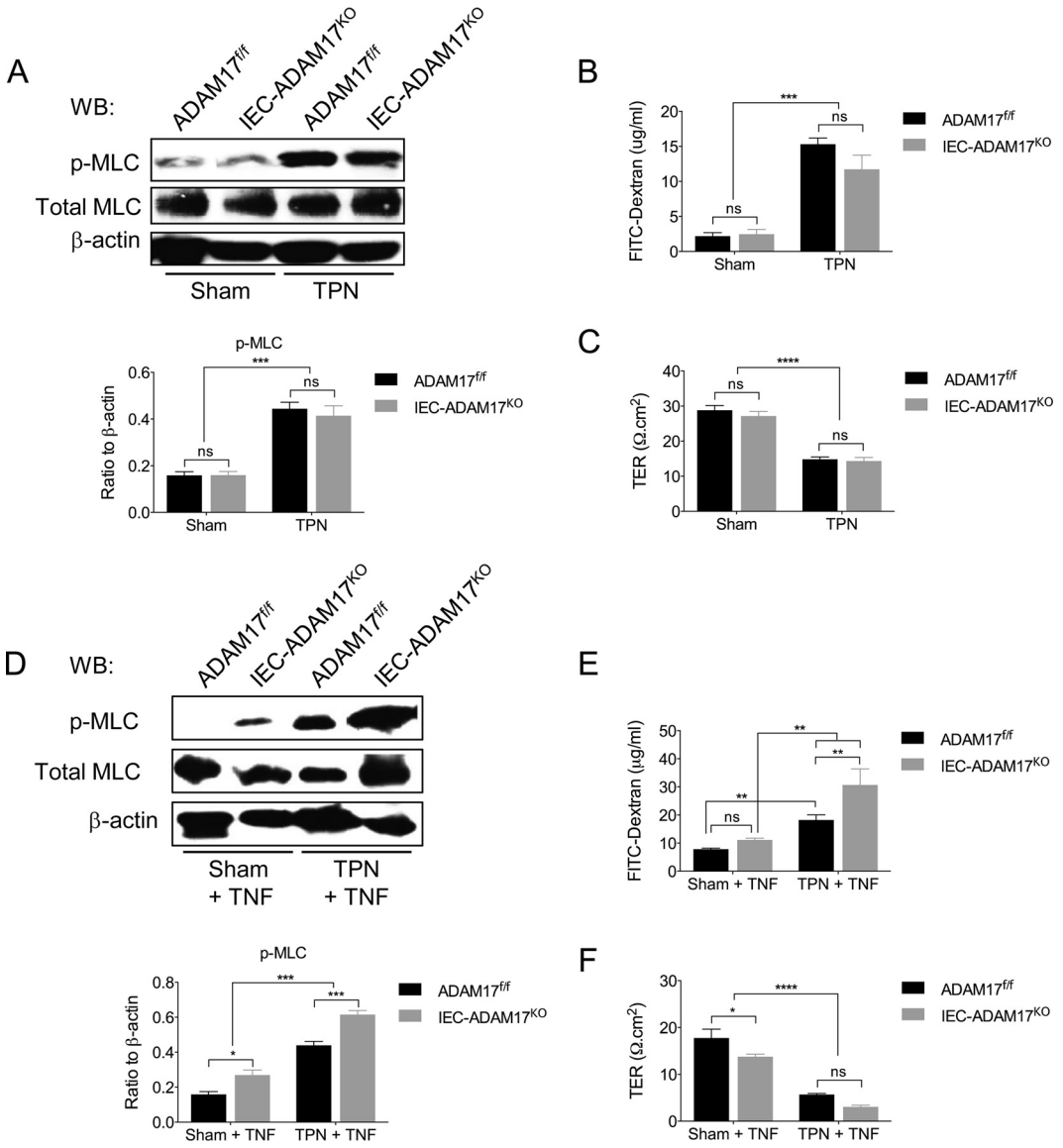

FIG 6 ADAM17 deletion does not improve EBF, but exogenous TNF-α treatment further impairs barrier dysfunction. EBF analysis at baseline (A to C) and after treatment with exogenous TNF-α (see Materials and Methods) (D to F). (A and D, top) Western blot analysis of p-MLC in isolated IECs. (Bottom) Quantification of p-MLC protein levels ($n = 4$ per group). (B and E) Paracellular permeability (panel B, $n = 7$ to 16 per group; panel E, $n = 5$ to 8 per group). (C and F) TER ($n = 5$ to 8 per group). *, $P < 0.05$; **, $P < 0.01$; ***, $P < 0.001$; ****, $P < 0.0001$; ns, not significant.

kines, these results suggest that the loss of ADAM17 signaling in IECs reduces local proinflammatory cytokine production and responses within the intestinal mucosa and this likely contributes to the amelioration of mucosal atrophy observed in TPN-treated *IEC-Adam17*^{KO} mice.

TPN-treated IEC-specific *Adam17*^{KO} mice maintain EGFR protein levels and downstream AKT and STAT3 signaling. TPN-induced TNFR signaling leads to loss of functional EGFR expression in IECs and the attenuation of mucosal atrophy observed in TPN-treated *TNFR1*^{KO} and *TNFR1R2*^{DKO} mice is directly dependent on the preservation of functional EGFR signaling (3). The importance of EGFR signaling is further illustrated by the ability of exogenous EGF to ameliorate mucosal atrophy in TPN-treated WT mice (3). Based on the observations that TPN-treated *IEC-Adam17*^{KO} mice have reduced sTNF-α signaling, we hypothesized that ADAM17 loss might restore functional EGFR signaling in IECs. To determine whether EGFR expression was altered by IEC-specific ADAM17 deficiency, we examined EGFR protein levels in IECs from sham and TPN-treated WT control and *IEC-Adam17*^{KO} mice. In TPN-treated WT mice, EGFR protein levels were markedly reduced in IECs compared to sham controls. In contrast, EGFR protein levels were partially restored in IECs from TPN-treated *IEC-Adam17*^{KO} mice (Fig. 8A and B), although it was still not possible to detect pEGFR under these experimental conditions (data not shown). Interestingly, while the mRNA expression of most EGFR/ErbB ligands (*Areg*, *Btc*, *Egf*, *Ereg*, *Tgfα*, *Nrg1*, *Nrg2*, and *Nrg3*) (see Fig. S1 in the supplemental material) in scraped mucosa was still diminished in TPN-treated *IEC-Adam17*^{KO} mice, the mRNA levels for *Hbegf* and to a lesser degree *Nrg4* were restored to baseline, suggesting that these two ligands

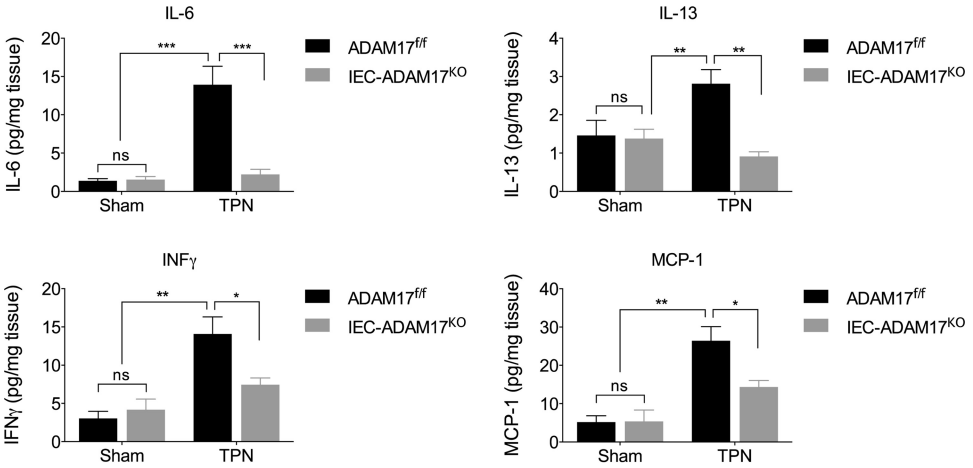

FIG 7 ADAM17 loss reduces cytokine protein levels in mucosal extracts upon TPN treatment. *, $P < 0.05$; **, $P < 0.01$; ***, $P < 0.001$; ns, not significant.

might also contribute to functional ErbB signaling in TPN-treated *IEC-Adam17*^{KO} mice (Fig. 8E).

In the TPN model, we have previously reported that activation of AKT and STAT3 are dependent of functional EGFR signaling, whereas phosphorylation of p38 MAPK requires functional TNFR1 signaling (see Fig. 6D) (3). To confirm that functional EGFR signaling was maintained in TPN-treated *IEC-Adam17*^{KO} mice, the levels of pAKT and pSTAT3 were measured in IECs from sham and TPN-treated WT control and *IEC-Adam17*^{KO} mice. Under sham treatment, WT control and *IEC-Adam17*^{KO} mice displayed similar levels of both phosphorylated proteins, indicating that IEC-specific ADAM17-deficiency did not significantly alter these downstream signaling events under baseline conditions. However, consistent with increased sTNF-α signaling and decreased EGFR protein levels seen after TPN administration, the pAKT and pSTAT3 protein levels were markedly reduced in the IECs of TPN-treated WT control mice. Importantly, and consistent with the restoration of EGFR protein levels, pAKT levels were restored to sham levels, while pSTAT3 levels were partially restored in IECs from TPN-treated *IEC-Adam17*^{KO} mice (Fig. 8A, C, and D).

Attenuation of mucosal atrophy in TPN-treated *IEC-Adam17*^{KO} mice is blocked by gefitinib. To further validate that maintenance of EGFR signaling was required for the beneficial IEC responses observed in TPN-treated *IEC-Adam17*^{KO} mice, the EGFR-specific kinase inhibitor, gefitinib was used to block EGFR signaling *in vivo*. Similar to TPN-treated *TNFR1*^{KO} mice receiving gefitinib (3), blockade of EGFR signaling in TPN-treated *IEC-Adam17*^{KO} mice exacerbated the mucosal atrophy with a significant reduction in crypt depth and villus height compared to vehicle controls (Fig. 9A). In addition, gefitinib treatment significantly reduced cell proliferation and PCNA levels, and increased apoptosis in IECs of TPN-treated *IEC-Adam17*^{KO} mice (Fig. 9B to D). Consistent with a loss of EGFR signaling, there was a concomitant and significant decrease in total EGFR and pAKT protein levels; however, pSTAT3 levels were unaltered, suggesting that ADAM17 regulation of pSTAT3 activity was EGFR independent (Fig. 9E). Interestingly, the reduced p-p38 MAPK levels observed in TPN-treated *IEC-Adam17*^{KO} mice were unaffected by gefitinib treatment which is in agreement with a continued loss of sTNF-α signaling in ADAM17-deficient mice (data not shown). Taken together, these results clearly demonstrate that retention of functional EGFR signaling is required for the improved IEC responses observed in TPN-treated *IEC-Adam17*^{KO} mice.

Mucosal atrophy in TPN-treated WT mice is attenuated by TNF-α blockade. Based on the above data, we hypothesized that increased TNF-α shedding by IECs from TPN-treated WT mice is an important early event responsible for reduced EGFR signaling in IECs and enhanced proinflammatory cytokine production leading to mucosal atrophy. However, conditional TNF-α-deficient mouse models are not currently available to directly test the role of IEC-specific TNF-α signaling in the TPN mouse model. In an alternative approach, we recently showed that treatment with the TNF-α inhibitor etanercept produced partial protection against TPN-associated epithelial barrier dysfunction (4). To extend these initial findings, we examined the effects of etanercept treatment on signaling events within the intestines of WT mice receiving TPN. As previously reported, TPN-treated WT mice given etanercept showed attenuated mucosal atrophy with improved crypt depth and villus height, enhanced epithelial barrier function (4) (data not shown) and increased crypt cell proliferation and PCNA protein levels (Fig. 10A to C). Moreover, etanercept treatment decreased IEC apoptosis in TPN-treated WT mice (Fig. 10D) which was associated with increased levels of the anti-apoptotic marker Bcl2, whereas Bax levels were unaltered (Fig. 10E). A similar decline in IEC apoptosis and increased Bcl2 levels were observed in TPN-treated *IEC-Adam17*^{KO} mice (Fig. 3B). The ability of etanercept to block sTNF-α signaling was confirmed by significant lowering of soluble TNF-α protein levels in mucosal extracts and serum of TPN-treated WT mice (Fig. 10F). Surprisingly, etanercept treatment did not alter the protein or mRNA levels of other proinflammatory cytokines (IFN-γ, MCP1, IL-13, and IL-6), although a modest increase in serum IL-6 levels was still observed (data not shown). Overall, these results clearly demonstrate that etanercept treatment blocked sTNF-α signaling and markedly improved intestinal function in TPN-treated WT mice.

Based on these observations, we hypothesized that the amelioration of mucosal atrophy observed upon TNF-α blockade should be associated with improved EGFR protein expression and enhanced downstream signaling. Consistent with a loss of sTNF-α signaling in these mice, both EGFR and pAKT proteins levels sig-

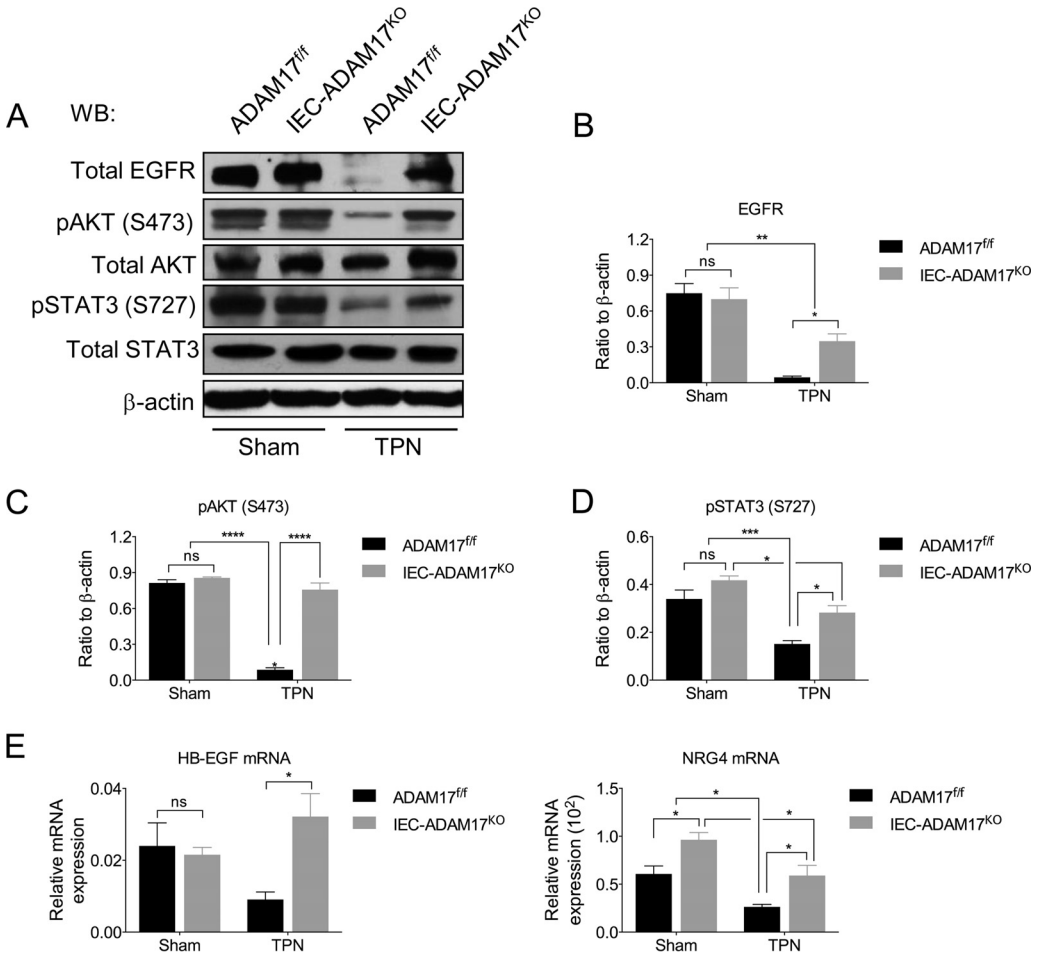

FIG 8 TPN-treated *IEC-Adam17*^{KO} mice have partially restored EGFR expression and improved downstream signaling. (A) Western blot analysis of EGFR, p-AKT, and p-STAT3, in isolated IECs. (B to D) Quantification of EGFR, p-AKT, and p-STAT3 protein levels, respectively ($n = 4$ to 6 per group). (E) Real-time PCR analysis of *Hbegf* and *Nrg4* mRNA expression in scraped mucosa ($n = 5$ to 8 per group). *, $P < 0.05$; **, $P < 0.01$; ***, $P < 0.001$; ****, $P < 0.0001$; ns, not significant.

nificantly increased in IECs after etanercept treatment in TPN-treated WT mice. Interestingly, and similar to gefitinib studies, TNF-α blockade did not modulate pSTAT3 levels, suggesting that ADAM17 regulation of pSTAT3 was also independent of TNF-α signaling (Fig. 10G). Restoration of functional EGFR signaling upon etanercept treatment was further supported by a marked recovery of mRNA levels for several EGFR/ErbB ligands, including those encoded by *Hbegf*, *Egf*, *Nrg1*, *Nrg2*, *Nrg3*, and *Nrg4* (see Fig. S2 in the supplemental material). Taken together, our findings are consistent with an important role of ADAM17 in regulating TNF-α signaling in IECs that is critical for early signaling events required for the detrimental IEC responses and mucosal atrophy produced by TPN administration.

DISCUSSION

Although TNF-α/TNFR signaling plays an important role in the development of TPN-induced mucosal atrophy, the tissue-specific contributions of TNF-α have not been defined (3, 4). In the present study, we used *IEC-Adam17*^{KO} mice to determine the effects of IEC-specific ADAM17 deficiency upon TPN-induced mucosal atrophy. Remarkably, mucosal atrophy was partially attenuated in TPN-treated *IEC-Adam17*^{KO} mice with improved intestinal length and crypt depth. This was accompanied with increased crypt cell proliferation, decreased IEC apoptosis, and reduced production of proinflammatory cytokines. Because ADAM17 can modulate TNF-α/TNFR and EGFR/ErbB signaling pathways, the effects of ADAM17 loss on both these pathways were examined in detail. Despite TPN administration increasing TNF-α mRNA levels, soluble TNF-α protein levels in mucosal extracts and serum were markedly reduced in TPN-treated *IEC-Adam17*^{KO} mice. A significant reduction of p-p38 MAPK signaling in IECs provided direct evidence that the overall soluble TNF-α signaling was decreased in the ADAM17-deficient state. Intriguingly, loss of soluble TNF-α signaling was observed even though the *IEC-Adam17*^{KO} mice displayed increased levels of functional TNFR receptors in IECs. This was clearly illustrated by the fact that TPN-treated *IEC-Adam17*^{KO} mice were hypersensitive to exogenous TNF-α, which markedly augmented barrier dysfunction in the ADAM17-deficient mice. Paradoxically, considering the role of ADAM17 in activating different EGFR/ErbB ligands, TPN-treated *IEC-Adam17*^{KO} mice showed partial restoration of EGFR protein levels in IECs and improved downstream pAKT signaling. EGFR kinase inhibitor studies confirmed that the

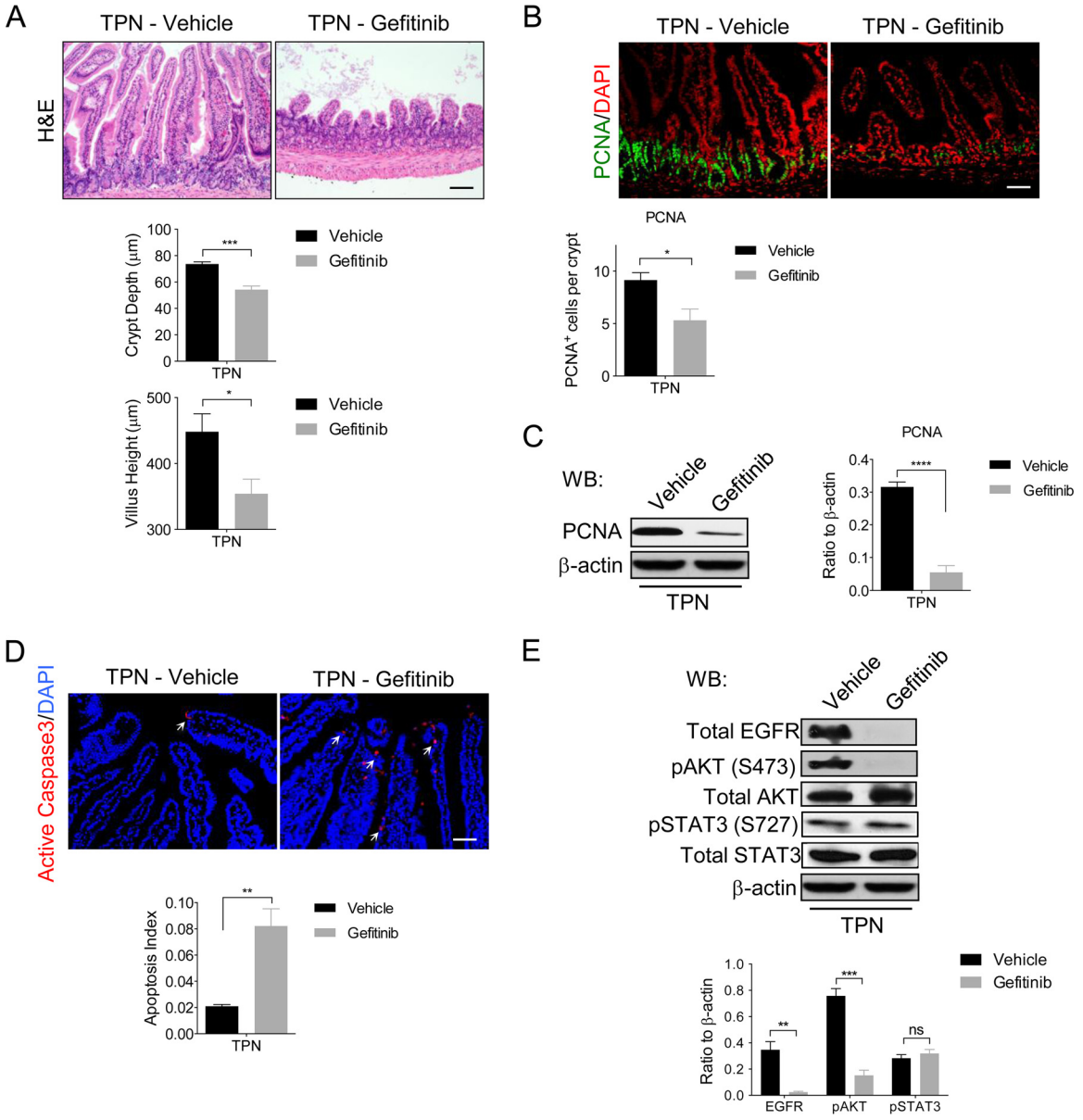

FIG 9 EGFR kinase inhibitor gefitinib blocks the beneficial effects of ADAM17 deficiency in TPN-treated mice. (A, top) H&E analysis. (Middle and bottom) Quantification of crypt depth and villus height ($n = 5$ per group). (B, top) Immunofluorescent staining for the cell proliferation marker, PCNA. (Bottom) Quantification of $PCNA^+$ cells per crypt ($n = 6$ to 8 per group). (C, left) Western blot analysis of PCNA in isolated IECs. (Right) Quantification of PCNA protein levels ($n = 3$ to 6 per group). (D, top) Immunofluorescence staining of active caspase-3. Arrows indicate caspase-3 staining. (Bottom) Quantification of apoptotic index ($n = 3$ or 4 per group). (E, top) Western blot analysis of EGFR, p-AKT, and p-STAT3 in isolated IECs. (Bottom) Quantification of EGFR, p-AKT, and p-STAT3 protein levels, respectively ($n = 4$ to 6 per group). Scale bars: panels A and B, 50 μm; panel D, 25 μm. *, $P < 0.05$; **, $P < 0.01$; ***, $P < 0.001$; ****, $P < 0.0001$; ns, not significant.

beneficial effects observed in TPN-treated *IEC-Adam17*^{KO} mice were dependent on functional EGFR signaling. Significantly, these results were validated using the TNF-α inhibitor etanercept in TPN-treated WT mice, which clearly showed that soluble TNF-α signaling had a critical role in the loss of functional EGFR signaling in IECs and the development of mucosal atrophy. Taken together, we conclude that ADAM17-mediated TNF-α signaling from IECs plays a significant and deleterious role in development of mucosal atrophy in mice deprived of enteral nutrition.

Previous reports of ADAM17 inactivation in the intestine have been limited to developmental studies with *Tace*$^{\Delta Zn/\Delta Zn}$ mice and a more recent description of two pediatric patients lacking ADAM17. Due to perinatal lethality, only the E17.5 intestinal phenotype of *Tace*$^{\Delta Zn/\Delta Zn}$ mice, which showed villus blunting and possible delayed epithelial maturation, has been described (11). Similarly, ADAM17-deficient pediatric patients were initially reported to have early onset diarrhea and intestinal inflammation associated with villus blunting and increased mononuclear infiltrates, but these features were variable and resolved over time (20). In contrast, hypomorphic ADAM17 mice are viable and show a

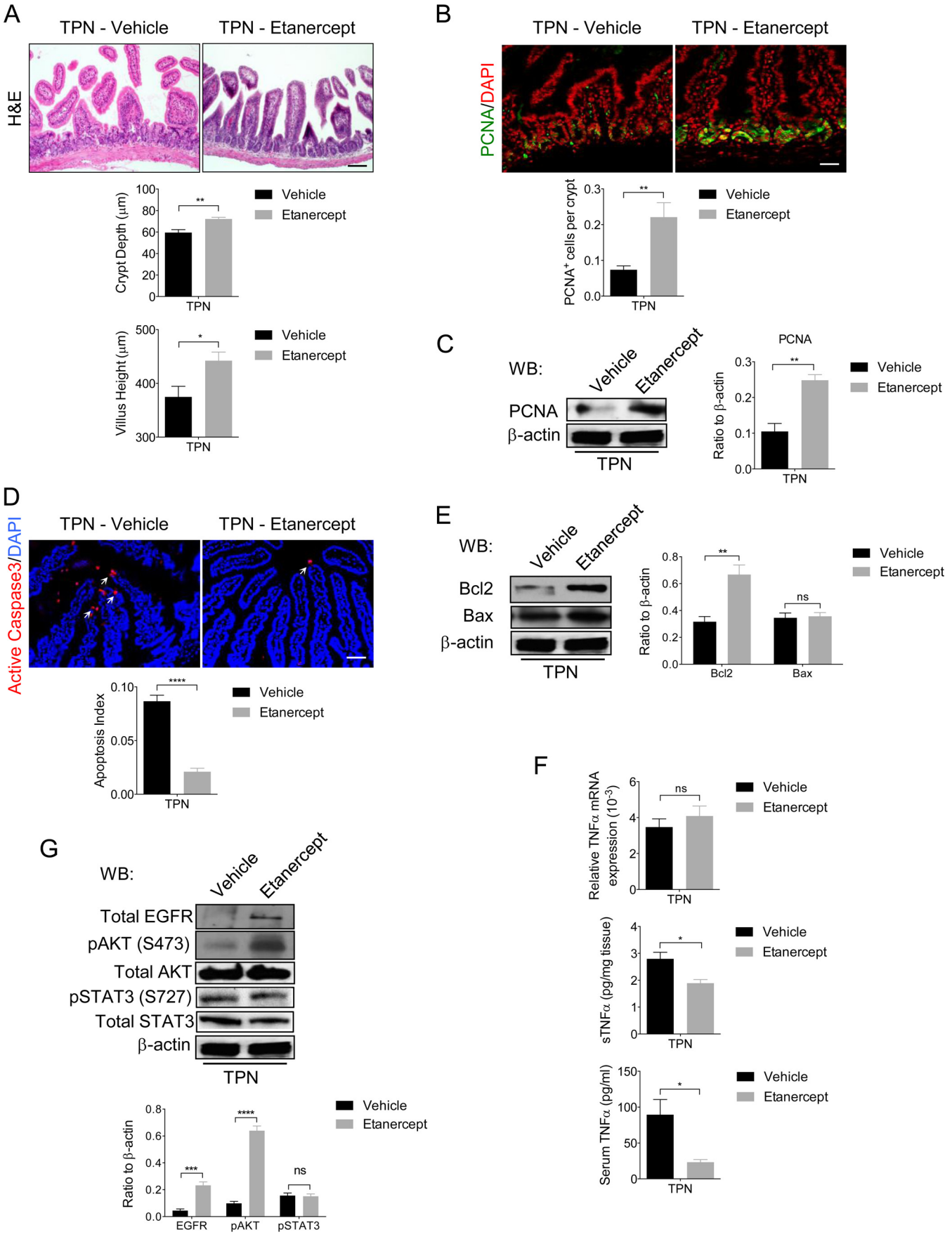
A
TPN - Vehicle
TPN - Etanercept
H&E
Crypt Depth (μm)
Villus Height (μm)
Vehicle
Etanercept
TPN
B
TPN - Vehicle
TPN - Etanercept
PCNA/DAPI
PCNA+ cells per crypt
C
WB:
Vehicle
Etanercept
PCNA
β-actin
Ratio to β-actin
D
TPN - Vehicle
TPN - Etanercept
Active Caspase3/DAPI
Apoptosis Index
E
WB:
Bcl2
Bax
β-actin
Ratio to β-actin
Bcl2
Bax
F
Relative TNFα mRNA expression (10-3)
sTNFα (pg/mg tissue)
Serum TNFα (pg/ml)
ns
G
WB:
Total EGFR
pAKT (S473)
Total AKT
pSTAT3 (S727)
Total STAT3
β-actin
Ratio to β-actin
EGFR
pAKT
pSTAT3

minimal intestinal phenotype but have a slightly enhanced proinflammatory cytokine gene signature (21, 23).

To investigate the role of ADAM17 deficiency in the intestine, we generated IEC-specific *Adam17*-deficient mice on a C57BL/6J genetic background. Under normal physiological conditions, adult *IEC-Adam17*^{KO} mice are overtly normal and show no significant changes in crypt-villus architecture, crypt proliferation and EBF. This finding is consistent with the lack of intestinal phenotype observed in different IEC-specific EGFR/ErbB-deficient mice (44, 45). Moreover, the normal secretory differentiation and viability of *IEC-Adam17*^{KO} mice suggests that ADAM17 is not essential for Notch signaling in IECs (37). The number and structure of Peyer's patches were also normal which is consistent with a role of TNF-α signaling in nonepithelial cells for the developmental organization of secondary lymphoid organs in the intestine (12, 46). In addition, intestinal cytokine expression in *IEC-Adam17*^{KO} mice was unaltered, suggesting that minimal perturbations in proinflammatory cytokine/immune status are present in these mice under normal physiological conditions. Taken together, these results indicate that *IEC-Adam17*^{KO} mouse model is a suitable model to investigate the contribution of ADAM17 signaling from IECs under different experimental conditions.

IEC proliferation is critical for adaptive growth after intestinal injury/inflammation (47, 48), and EGFR/ErbB is a major mediator of these IEC responses (44, 48, 49). In the DSS colitis model, hypomorphic *Egfr* mice and ErbB ligand-deficient mice display exacerbated intestinal inflammation (50, 51), whereas more recent studies using different *IEC-ErbB*^{KO} mice have shown that all four ErbB receptors contribute, in various degrees, to protection against DSS-induced colitis (19, 24, 26, 45). Evidence that ADAM17 is an upstream regulator of EGFR/ErbB signaling in the DSS colitis model comes from analysis of hypomorphic *Adam17* mice under continuous exposure to low-dose DSS (21, 23). Hypomorphic *Adam17* mice showed increased susceptibility to DSS-induced colitis but these mice could be protected by treatment with exogenous ErbB ligands (21, 23). Interestingly, our own preliminary experiments with *IEC-Adam17*^{KO} mice in the DSS colitis model have demonstrated that a loss of ADAM17 in IECs exacerbates DSS-induced epithelial cell injury (data not shown) (52). In studies of hypomorphic *Adam17* mice, Brandl et al. showed that DSS-induced colitis activated TLR-mediated MyD88 signaling which dramatically increased expression of two ErbB ligands, *Areg* and *Ereg*. Because *Areg* and *Ereg* are both ADAM17 substrates (53), it has been postulated that ADAM17-mediated ErbB ligand shedding to produce soluble ligands plays critical role in activating ErbB signaling in IECs (21). Although the cellular source of these ErbB ligands was not clearly defined in this study, other studies have highlighted the contribution of ErbB ligand/EGFR signaling axis from nonepithelial mucosal cell types, including myeloid/immune cells and pericryptal myofibroblasts found in the lamina propria (54, 55).

Intriguingly, and in direct contrast to increased susceptibility of ADAM17-deficient mice to DSS-induced colitis, mucosal atrophy was attenuated in TPN-treated *IEC-Adam17*^{KO} mice. The dramatic difference in IEC responses by *IEC-Adam17*^{KO} mice in these two models is likely due to the importance of soluble TNF-α signaling in IEC signaling events, leading to mucosal atrophy in TPN-treated mice, whereas ErbB signaling in IECs is cytoprotective against IEC injury in the DSS colitis model. We have previously shown that increased TNF-α/TNFR1 signaling was responsible for mucosal atrophy, as well as reduced IEC proliferation and increased IEC apoptosis observed upon TPN administration (3). In TNFR1-deficient mice, the protection against TPN-associated mucosal atrophy was dependent on the restoration of EGFR signaling highlighting an interdependence of TNFR1 and EGFR signaling for this response (3). Similarly, an overall improvement in IEC responses in TPN-treated *IEC-Adam17*^{KO} mice was associated decreased soluble TNF-α signaling, a marked reduction in proinflammatory cytokine production and retention of EGFR signaling in IECs. Mechanistically, our results are consistent with several recent studies showing that TNF-α/TNFR1-mediated p38 MAPK signaling can induce EGFR internalization and downregulate EGFR signaling in IECs (56–58). The reduced soluble TNF-α levels and decreased p38 MAPK signaling in IECs observed in TPN-treated *IEC-Adam17*^{KO} mice is therefore a likely explanation for the restoration of EGFR protein levels and increased pAKT signaling in IECs. The importance of functional EGFR signaling for the amelioration of mucosal atrophy observed in TPN-treated *IEC-Adam17*^{KO} mice is clearly demonstrated by the ability of the EGFR kinase inhibitor gefitinib to block the beneficial IEC responses in these mice. Moreover, administration of TNF-α inhibitor etanercept to TPN-treated WT mice confirmed that TNF-α blockade was required for restoration of EGFR protein levels and improved IEC responses in an EGFR-dependent manner. Although these results suggest a critical role of soluble TNF-α signaling in the development of TPN-induced mucosal atrophy, lymphotoxin-α, which signals through TNFR1 and is also neutralized by etanercept, may also contribute to this process (12, 59).

Considering that shedding and activation of many ErbB ligands is ADAM17 dependent (53), it was surprising to demonstrate that the improved IECs responses observed in TPN-treated *IEC-Adam17*^{KO} mice were reliant on functional EGFR signaling in IECs. Analysis of ErbB ligand mRNA expression in scraped mucosa from TPN-treated *IEC-Adam17*^{KO} mice showed that only *Hbegf* and *Nrg4* mRNA levels were restored to near baseline levels, whereas the expression of all other ErbB ligands remained suppressed in the ADAM17-deficient state. In spite of continued ErbB ligand mRNA suppression and decreased production of active ErbB ligands from IECs, functional EGFR signaling in IECs was still critical for the beneficial IEC responses observed in TPN-treated *IEC-Adam17*^{KO} mice. Although IEC expression of ADAM10-dependent ErbB ligands such as EGF may contribute to

FIG 10 Etanercept attenuates mucosal atrophy and improves EGFR signaling in IECs upon TPN administration. (A, top) H&E analysis. (Middle and bottom) Quantification of crypt depth and villus height ($n = 5$ per group). (B, top) Immunofluorescence staining of the cell proliferation marker, PCNA. (Bottom) Quantification of PCNA$^+$ cells per crypt ($n = 5$ per group). (C, left) Western blot analysis of PCNA in isolated IECs. (Right) Quantification of PCNA protein levels ($n = 3$ to 6 per group). (D, top) Immunofluorescence staining of the apoptotic cell marker, active caspase-3. Arrows indicate caspase-3 staining. (Bottom) Quantification of apoptotic index ($n = 5$ per group). (E, left) Western blot analysis of Bcl-2 and Bax in isolated IECs ($n = 4$ or 5 per group). (Right) Quantification of Bcl2 and Bax protein levels. (F) The results of real-time PCR analysis of TNF-α mRNA expression in scraped mucosa (top) and sTNF-α protein levels in scraped mucosa (middle) and serum (bottom) ($n = 5$ or 6 per group). (G, top) Western blot analysis of EGFR, p-AKT, and pSTAT3 in isolated IECs. (Bottom) Quantification of EGFR, p-AKT, and p-STAT3 protein levels, respectively. Scale bars: panel A, 50 μm; panels B and D, 25 μm. *, $P < 0.05$; **, $P < 0.01$; ***, $P < 0.001$; ****, $P < 0.0001$; ns, not significant.

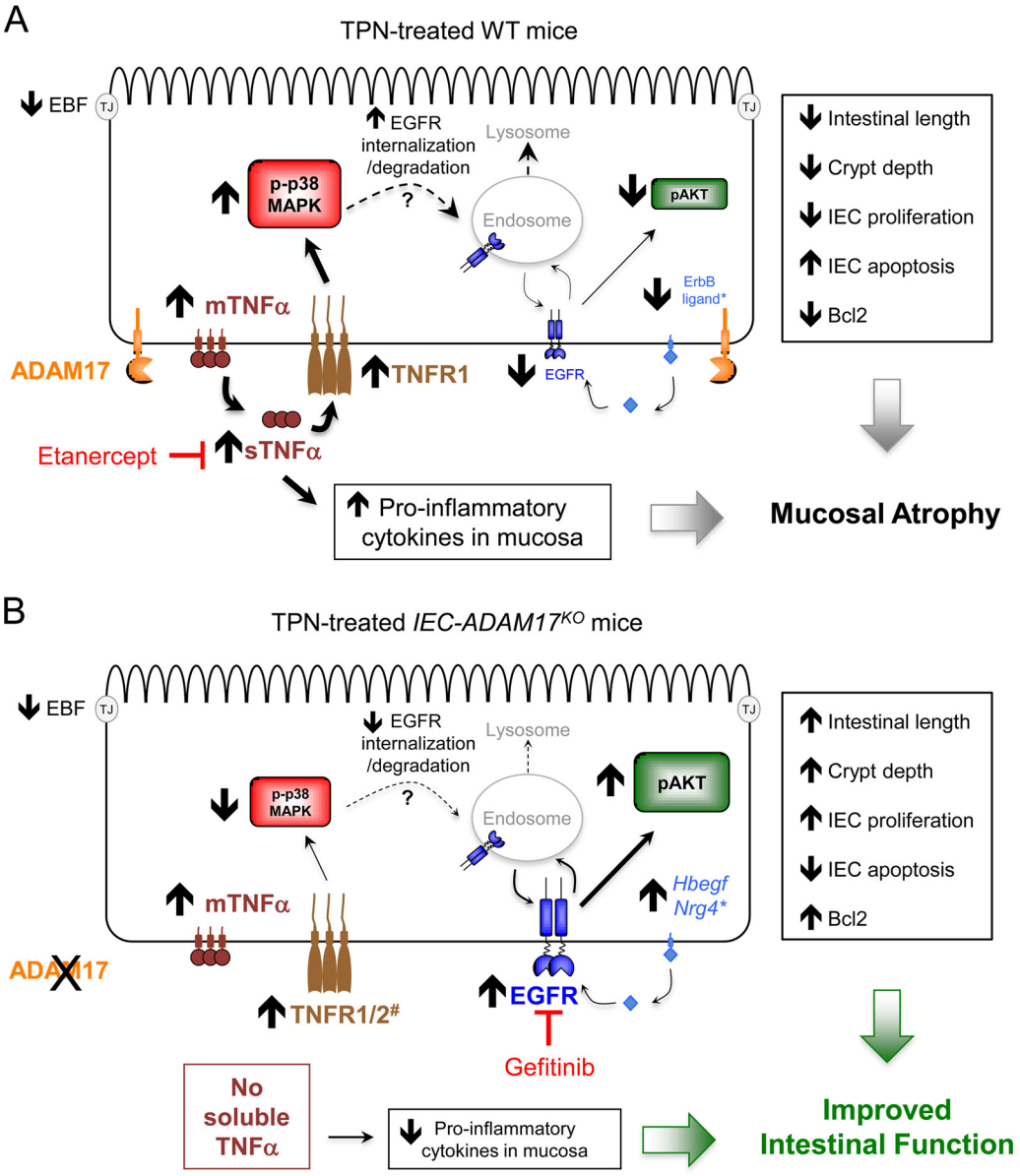

FIG 11 Model for ADAM17-mediated TNF-α signaling in IECs and the development of TPN-induced mucosal atrophy. (A) In TPN-treated wild-type (WT) mice, the TNF-α and TNFR1 mRNA and protein levels are upregulated in IECs, leading to increased production of soluble TNF-α, increased TNFR1 signaling, and activation of p-p38-MAPK in IECs. There is a concomitant reduction in EGFR protein levels and decreased functional pAKT signaling in IECs. *, EGFR signaling is further compromised by reduced ErbB ligand mRNA expression within the intestinal mucosa. Etanercept blocks soluble TNF-α signaling, leading to reduced p38-MAPK signaling in IECs. There is a concomitant restoration of EGFR protein levels and functional pAKT signaling in IECs. (B) In TPN-treated *IEC-ADAM17*^{KO} mice, TNF-α and TNFR1 mRNA and protein levels are upregulated in IECs. However, there is no generation of soluble TNF-α leading to reduced TNFR1 and p-p38-MAPK signaling in IECs. #, ADAM17 deficiency also increases TNFR2 cell surface protein levels, which may alter the balance of TNFR signaling in IECs. Despite the loss of ADAM17-mediated ErbB ligand shedding in IECs, there is a partial restoration of EGFR protein levels and functional pAKT signaling in IECs. *, increased *Hbegf* and *Nrg4* mRNA levels in the intestinal mucosa may contribute to this process. Gefitinib blocks these protective effects confirming the importance of functional EGFR signaling in the attenuation of mucosal atrophy observed in TPN-treated *IEC-ADAM17*^{KO} mice.

autocrine EGFR signaling in IECs (53), several studies have recently highlighted the importance of ErbB ligand production and EGFR signaling from nonepithelial cell types during intestinal inflammation and tumorigenesis (54, 55). Thus, a more likely scenario is that the principal source of soluble ErbB ligands, including HB-EGF and NRG4, is from cell types within the lamina propria that still express ADAM17 and act in a paracrine manner. Further studies will be needed to address whether immune cells or mesenchymally derived cells such as pericryptal myofibroblasts are the principal source of these ErbB ligands.

IECs are critical for regulating intestinal immune responses to inflammation and injury but only recently has the importance of cytokine/chemokine production from IECs been established (59–63). Roulis et al. showed recently that TNF-α overexpression in IECs is responsible for Crohn's-like symptoms observed in *Tnf*$^{(\Delta ARE/+)}$ mice. Interestingly, the intestinal inflammation ob-

served in this model did not require autocrine TNF-α/TNFR1 signaling within IECs but instead was triggered by paracrine TNF-α signaling and activation of myofibroblasts (60). In the present study, we have demonstrated for the first time that endogenous TNF-α production from IECs is crucial for the deleterious IEC responses associated with TPN-induced mucosal atrophy. We propose that ADAM17-dependent shedding of TNF-α from IECs is a critical initiating event in the development and progression of the proinflammatory response within the intestine of TPN-treated mice. A summary of the role of ADAM17 in regulating TNF-α/TNFR and ErbB ligand/EGFR signaling pathways within IECs of the mouse TPN model is shown in Fig. 11. Anti-TNF-α therapies have been successfully used to treat patients with inflammatory bowel disease (59, 63). The data from the present study suggest that inhibition of the ADAM17/TNF-α signaling axis may also be a potential therapeutic option for patients dependent on TPN.

ACKNOWLEDGMENTS

This study was supported by National Institutes of Health grants R01-DK093697 (P.J.D.), R01-AI044076 (D.H.T.), and RO1-HL067267 (E.W.R.). This study utilized the Morphology and Image Analysis Core of the Michigan Diabetes Research Center funded by the National Institute of Diabetes and Digestive and Kidney Diseases (P60DK020572).

We thank Shelly Rustagi and Jennifer Jones for critically reading the manuscript.

REFERENCES

1. **Demehri FR, Barrett M, Ralls MW, Miyasaka EA, Feng Y, Teitelbaum DH.** 2013. Intestinal epithelial cell apoptosis and loss of barrier function in the setting of altered microbiota with enteral nutrient deprivation. Front Cell Infect Microbiol **3:**105. http://dx.doi.org/10.3389/fcimb.2013.00105.
2. **Casaer MP, Mesotten D, Hermans G, Wouters PJ, Schetz M, Meyfroidt G, Van Cromphaut S, Ingels C, Meersseman P, Muller J, Vlasselaers D, Debaveye Y, Desmet L, Dubois J, Van Assche A, Vanderheyden S, Wilmer A, Van den Berghe G.** 2011. Early versus late parenteral nutrition in critically ill adults. N Engl J Med **365:**506–517. http://dx.doi.org/10.1056/NEJMoa1102662.
3. **Feng Y, Teitelbaum DH.** 2012. Epidermal growth factor/TNF-alpha transactivation modulates epithelial cell proliferation and apoptosis in a mouse model of parenteral nutrition. Am J Physiol Gastrointest Liver Physiol **302:**G236–G249. http://dx.doi.org/10.1152/ajpgi.00142.2011.
4. **Feng Y, Teitelbaum DH.** 2013. Tumour necrosis factor–induced loss of intestinal barrier function requires TNFR1 and TNFR2 signaling in a mouse model of total parenteral nutrition. J Physiol **591:**3709–3723. http://dx.doi.org/10.1113/jphysiol.2013.253518.
5. **Scheller J, Chalaris A, Garbers C, Rose-John S.** 2011. ADAM17: a molecular switch to control inflammation and tissue regeneration. Trends Immunol **32:**380–387. http://dx.doi.org/10.1016/j.it.2011.05.005.
6. **Weber S, Saftig P.** 2012. Ectodomain shedding and ADAMs in development. Development **139:**3693–3709. http://dx.doi.org/10.1242/dev.076398.
7. **Moss ML, Jin SL, Milla ME, Bickett DM, Burkhart W, Carter HL, Chen WJ, Clay WC, Didsbury JR, Hassler D, Hoffman CR, Kost TA, Lambert MH, Leesnitzer MA, McCauley P, McGeehan G, Mitchell J, Moyer M, Pahel G, Rocque W, Overton LK, Schoenen F, Seaton T, Su JL, Becherer JD, et al.** 1997. Cloning of a disintegrin metalloproteinase that processes precursor tumour-necrosis factor-alpha. Nature **385:**733–736. http://dx.doi.org/10.1038/385733a0.
8. **Black RA, Rauch CT, Kozlosky CJ, Peschon JJ, Slack JL, Wolfson MF, Castner BJ, Stocking KL, Reddy P, Srinivasan S, Nelson N, Boiani N, Schooley KA, Gerhart M, Davis R, Fitzner JN, Johnson RS, Paxton RJ, March CJ, Cerretti DP.** 1997. A metalloproteinase disintegrin that releases tumour-necrosis factor-alpha from cells. Nature **385:**729–733. http://dx.doi.org/10.1038/385729a0.
9. **Bell JH, Herrera AH, Li Y, Walcheck B.** 2007. Role of ADAM17 in the ectodomain shedding of TNF-alpha and its receptors by neutrophils and macrophages. J Leukoc Biol **82:**173–176. http://dx.doi.org/10.1189/jlb.0307193.
10. **Li N, Boyd K, Dempsey PJ, Vignali DA.** 2007. Non-cell autonomous expression of TNF-alpha-converting enzyme ADAM17 is required for normal lymphocyte development. J Immunol **178:**4214–4221. http://dx.doi.org/10.4049/jimmunol.178.7.4214.
11. **Peschon JJ, Slack JL, Reddy P, Stocking KL, Sunnarborg SW, Lee DC, Russell WE, Castner BJ, Johnson RS, Fitzner JN, Boyce RW, Nelson N, Kozlosky CJ, Wolfson MF, Rauch CT, Cerretti DP, Paxton RJ, March CJ, Black RA.** 1998. An essential role for ectodomain shedding in mammalian development. Science **282:**1281–1284. http://dx.doi.org/10.1126/science.282.5392.1281.
12. **Winsauer C, Kruglov AA, Chashchina AA, Drutskaya MS, Nedospasov SA.** 2014. Cellular sources of pathogenic and protective TNF and experimental strategies based on utilization of TNF humanized mice. Cytokine Growth Factor Rev **25:**115–123. http://dx.doi.org/10.1016/j.cytogfr.2013.12.005.
13. **Li N, Wang Y, Forbes K, Vignali KM, Heale BS, Saftig P, Hartmann D, Black RA, Rossi JJ, Blobel CP, Dempsey PJ, Workman CJ, Vignali DA.** 2007. Metalloproteases regulate T-cell proliferation and effector function via LAG-3. EMBO J **26:**494–504. http://dx.doi.org/10.1038/sj.emboj.7601520.
14. **Sibilia M, Wagner EF.** 1995. Strain-dependent epithelial defects in mice lacking the EGF receptor. Science **269:**234–238. http://dx.doi.org/10.1126/science.7618085.
15. **Threadgill DW, Dlugosz AA, Hansen LA, Tennenbaum T, Lichti U, Yee D, LaMantia C, Mourton T, Herrup K, Harris RC, et al.** 1995. Targeted disruption of mouse EGF receptor: effect of genetic background on mutant phenotype. Science **269:**230–234. http://dx.doi.org/10.1126/science.7618084.
16. **Mann GB, Fowler KJ, Gabriel A, Nice EC, Williams RL, Dunn AR.** 1993. Mice with a null mutation of the TGF alpha gene have abnormal skin architecture, wavy hair, and curly whiskers and often develop corneal inflammation. Cell **73:**249–261. http://dx.doi.org/10.1016/0092-8674(93)90227-H.
17. **Sternlicht MD, Sunnarborg SW, Kouros-Mehr H, Yu Y, Lee DC, Werb Z.** 2005. Mammary ductal morphogenesis requires paracrine activation of stromal EGFR via ADAM17-dependent shedding of epithelial amphiregulin. Development **132:**3923–3933. http://dx.doi.org/10.1242/dev.01966.
18. **Jackson LF, Qiu TH, Sunnarborg SW, Chang A, Zhang C, Patterson C, Lee DC.** 2003. Defective valvulogenesis in HB-EGF and TACE-null mice is associated with aberrant BMP signaling. EMBO J **22:**2704–2716. http://dx.doi.org/10.1093/emboj/cdg264.
19. **Franzke CW, Cobzaru C, Triantafyllopoulou A, Loffek S, Horiuchi K, Threadgill DW, Kurz T, van Rooijen N, Bruckner-Tuderman L, Blobel CP.** 2012. Epidermal ADAM17 maintains the skin barrier by regulating EGFR ligand-dependent terminal keratinocyte differentiation. J Exp Med **209:**1105–1119. http://dx.doi.org/10.1084/jem.20112258.
20. **Blaydon DC, Biancheri P, Di WL, Plagnol V, Cabral RM, Brooke MA, van Heel DA, Ruschendorf F, Toynbee M, Walne A, O'Toole EA, Martin JE, Lindley K, Vulliamy T, Abrams DJ, MacDonald TT, Harper JI, Kelsell DP.** 2011. Inflammatory skin and bowel disease linked to ADAM17 deletion. N Engl J Med **365:**1502–1508. http://dx.doi.org/10.1056/NEJMoa1100721.
21. **Brandl K, Sun L, Neppl C, Siggs OM, Le Gall SM, Tomisato W, Li X, Du X, Maennel DN, Blobel CP, Beutler B.** 2010. MyD88 signaling in nonhematopoietic cells protects mice against induced colitis by regulating specific EGF receptor ligands. Proc Natl Acad Sci U S A **107:**19967–19972. http://dx.doi.org/10.1073/pnas.1014669107.
22. **Brandl K, Tomisato W, Beutler B.** 2012. Inflammatory bowel disease and ADAM17 deletion. N Engl J Med **366:**190. http://dx.doi.org/10.1056/NEJMc1113373.
23. **Chalaris A, Adam N, Sina C, Rosenstiel P, Lehmann-Koch J, Schirmacher P, Hartmann D, Cichy J, Gavrilova O, Schreiber S, Jostock T, Matthews V, Hasler R, Becker C, Neurath MF, Reiss K, Saftig P, Scheller J, Rose-John S.** 2010. Critical role of the disintegrin metalloprotease ADAM17 for intestinal inflammation and regeneration in mice. J Exp Med **207:**1617–1624. http://dx.doi.org/10.1084/jem.20092366.
24. **Frey MR, Edelblum KL, Mullane MT, Liang D, Polk DB.** 2009. The ErbB4 growth factor receptor is required for colon epithelial cell survival in the presence of TNF. Gastroenterology **136:**217–226. http://dx.doi.org/10.1053/j.gastro.2008.09.023.
25. **Hobbs SS, Goettel JA, Liang D, Yan F, Edelblum KL, Frey MR, Mullane MT, Polk DB.** 2011. TNF transactivation of EGFR stimulates cytoprotec-

tive COX-2 expression in gastrointestinal epithelial cells. Am J Physiol Gastrointest Liver Physiol **301:**G220–G229. http://dx.doi.org/10.1152/ajpgi.00383.2010.
26. **Zhang Y, Dube PE, Washington MK, Yan F, Polk DB.** 2012. ErbB2 and ErbB3 regulate recovery from dextran sulfate sodium-induced colitis by promoting mouse colon epithelial cell survival. Lab Invest **92:**437–450. http://dx.doi.org/10.1038/labinvest.2011.192.
27. **el Marjou F, Janssen KP, Chang BH, Li M, Hindie V, Chan L, Louvard D, Chambon P, Metzger D, Robine S.** 2004. Tissue-specific and inducible Cre-mediated recombination in the gut epithelium. Genesis **39:**186–193. http://dx.doi.org/10.1002/gene.20042.
28. **Tang J, Zarbock A, Gomez I, Wilson CL, Lefort CT, Stadtmann A, Bell B, Huang LC, Ley K, Raines EW.** 2011. Adam17-dependent shedding limits early neutrophil influx but does not alter early monocyte recruitment to inflammatory sites. Blood **118:**786–794. http://dx.doi.org/10.1182/blood-2010-11-321406.
29. **Wilson CL, Gough PJ, Chang CA, Chan CK, Frey JM, Liu Y, Braun KR, Chin MT, Wight TN, Raines EW.** 2013. Endothelial deletion of ADAM17 in mice results in defective remodeling of the semilunar valves and cardiac dysfunction in adults. Mech Dev **130:**272–289. http://dx.doi.org/10.1016/j.mod.2013.01.001.
30. **Yan F, Liu L, Dempsey PJ, Tsai YH, Raines EW, Wilson CL, Cao H, Cao Z, Liu L, Polk DB.** 2013. A *Lactobacillus rhamnosus* GG-derived soluble protein, p40, stimulates ligand release from intestinal epithelial cells to transactivate epidermal growth factor receptor. J Biol Chem **288:**30742–30751. http://dx.doi.org/10.1074/jbc.M113.492397.
31. **Yang H, Madison B, Gumucio DL, Teitelbaum DH.** 2008. Specific overexpression of IL-7 in the intestinal mucosa: the role in intestinal intraepithelial lymphocyte development. Am J Physiol Gastrointest Liver Physiol **294:**G1421–G1430. http://dx.doi.org/10.1152/ajpgi.00060.2008.
32. **Zhang C, Feng Y, Yang H, Koga H, Teitelbaum DH.** 2009. The bone morphogenetic protein signaling pathway is upregulated in a mouse model of total parenteral nutrition. J Nutr **139:**1315–1321. http://dx.doi.org/10.3945/jn.108.096669.
33. **Karaman MW, Herrgard S, Treiber DK, Gallant P, Atteridge CE, Campbell BT, Chan KW, Ciceri P, Davis MI, Edeen PT, Faraoni R, Floyd M, Hunt JP, Lockhart DJ, Milanov ZV, Morrison MJ, Pallares G, Patel HK, Pritchard S, Wodicka LM, Zarrinkar PP.** 2008. A quantitative analysis of kinase inhibitor selectivity. Nat Biotechnol **26:**127–132. http://dx.doi.org/10.1038/nbt1358.
34. **Fries W, Muja C, Crisafulli C, Costantino G, Longo G, Cuzzocrea S, Mazzon E.** 2008. Infliximab and etanercept are equally effective in reducing enterocyte APOPTOSIS in experimental colitis. Int J Med Sci **5:**169–180.
35. **Nemoto H, Konno S, Sugimoto H, Nakazora H, Nomoto N, Murata M, Kitazono H, Fujioka T.** 2011. Anti-TNF therapy using etanercept suppresses degenerative and inflammatory changes in skeletal muscle of older SJL/J mice. Exp Mol Pathol **90:**264–270. http://dx.doi.org/10.1016/j.yexmp.2011.02.003.
36. **Gunther C, Martini E, Wittkopf N, Amann K, Weigmann B, Neumann H, Waldner MJ, Hedrick SM, Tenzer S, Neurath MF, Becker C.** 2011. Caspase-8 regulates TNF-alpha-induced epithelial necroptosis and terminal ileitis. Nature **477:**335–339. http://dx.doi.org/10.1038/nature10400.
37. **Tsai YH, VanDussen KL, Sawey ET, Wade AW, Kasper C, Rakshit S, Bhatt RG, Stoeck A, Maillard I, Crawford HC, Samuelson LC, Dempsey PJ.** 2014. ADAM10 regulates Notch function in intestinal stem cells of mice. Gastroenterology **147:**822–834. http://dx.doi.org/10.1053/j.gastro.2014.07.003.
38. **Feng Y, McDunn JE, Teitelbaum DH.** 2010. Decreased phospho-Akt signaling in a mouse model of total parenteral nutrition: a potential mechanism for the development of intestinal mucosal atrophy. Am J Physiol Gastrointest Liver Physiol **298:**G833–G841. http://dx.doi.org/10.1152/ajpgi.00030.2010.
39. **Yang H, Kiristioglu I, Fan Y, Forbush B, Bishop DK, Antony PA, Zhou H, Teitelbaum DH.** 2002. Interferon-gamma expression by intraepithelial lymphocytes results in a loss of epithelial barrier function in a mouse model of total parenteral nutrition. Ann Surg **236:**226–234. http://dx.doi.org/10.1097/00000658-200208000-00011.
40. **Yang H, Fan Y, Teitelbaum DH.** 2003. Intraepithelial lymphocyte-derived interferon-gamma evokes enterocyte apoptosis with parenteral nutrition in mice. Am J Physiol Gastrointest Liver Physiol **284:**G629–G637. http://dx.doi.org/10.1152/ajpgi.00290.2002.
41. **Sun X, Yang H, Nose K, Nose S, Haxhija EQ, Koga H, Feng Y, Teitelbaum DH.** 2008. Decline in intestinal mucosal IL-10 expression and decreased intestinal barrier function in a mouse model of total parenteral nutrition. Am J Physiol Gastrointest Liver Physiol **294:**G139–G147.
42. **Miyasaka EA, Feng Y, Poroyko V, Falkowski NR, Erb-Downward J, Gillilland MG, III, Mason KL, Huffnagle GB, Teitelbaum DH.** 2013. Total parenteral nutrition-associated lamina propria inflammation in mice is mediated by a MyD88-dependent mechanism. J Immunol **190:**6607–6615. http://dx.doi.org/10.4049/jimmunol.1201746.
43. **Grivennikov S, Karin E, Terzic J, Mucida D, Yu GY, Vallabhapurapu S, Scheller J, Rose-John S, Cheroutre H, Eckmann L, Karin M.** 2009. IL-6 and Stat3 are required for survival of intestinal epithelial cells and development of colitis-associated cancer. Cancer Cell **15:**103–113. http://dx.doi.org/10.1016/j.ccr.2009.01.001.
44. **Rowland KJ, McMellen ME, Wakeman D, Wandu WS, Erwin CR, Warner BW.** 2012. Enterocyte expression of epidermal growth factor receptor is not required for intestinal adaptation in response to massive small bowel resection. J Pediatr Surg **47:**1748–1753. http://dx.doi.org/10.1016/j.jpedsurg.2012.03.089.
45. **Yan F, Cao H, Cover TL, Washington MK, Shi Y, Liu L, Chaturvedi R, Peek RM, Jr, Wilson KT, Polk DB.** 2011. Colon-specific delivery of a probiotic-derived soluble protein ameliorates intestinal inflammation in mice through an EGFR-dependent mechanism. J Clin Invest **121:**2242–2253. http://dx.doi.org/10.1172/JCI44031.
46. **Kruglov AA, Kuchmiy A, Grivennikov SI, Tumanov AV, Kuprash DV, Nedospasov SA.** 2008. Physiological functions of tumor necrosis factor and the consequences of its pathologic overexpression or blockade: mouse models. Cytokine Growth Factor Rev **19:**231–244. http://dx.doi.org/10.1016/j.cytogfr.2008.04.010.
47. **Dekaney CM, Gulati AS, Garrison AP, Helmrath MA, Henning SJ.** 2009. Regeneration of intestinal stem/progenitor cells following doxorubicin treatment of mice. Am J Physiol Gastrointest Liver Physiol **297:**G461–G470. http://dx.doi.org/10.1152/ajpgi.90446.2008.
48. **Helmrath MA, Shin CE, Erwin CR, Warner BW.** 1998. The EGF\EGF-receptor axis modulates enterocyte apoptosis during intestinal adaptation. J Surg Res **77:**17–22. http://dx.doi.org/10.1006/jsre.1998.5362.
49. **Krishnan K, Arnone B, Buchman A.** 2011. Intestinal growth factors: potential use in the treatment of inflammatory bowel disease and their role in mucosal healing. Inflamm Bowel Dis **17:**410–422. http://dx.doi.org/10.1002/ibd.21316.
50. **Egger B, Buchler MW, Lakshmanan J, Moore P, Eysselein VE.** 2000. Mice harboring a defective epidermal growth factor receptor (waved-2) have an increased susceptibility to acute dextran sulfate-induced colitis. Scand J Gastroenterol **35:**1181–1187. http://dx.doi.org/10.1080/003655200750056664.
51. **Egger B, Procaccino F, Lakshmanan J, Reinshagen M, Hoffmann P, Patel A, Reuben W, Gnanakkan S, Liu L, Barajas L, Eysselein VE.** 1997. Mice lacking transforming growth factor alpha have an increased susceptibility to dextran sulfate-induced colitis. Gastroenterology **113:**825–832. http://dx.doi.org/10.1016/S0016-5085(97)70177-X.
52. **Tsai Y-H, Feng Y, Wade A, Teitelbaum D, Dempsey P.** 2012. Intestinal cell responses in different injury/regeneration models are differentially dependent on ADAM17. Gastroenterology **142:**S-61.
53. **Sahin U, Weskamp G, Kelly K, Zhou HM, Higashiyama S, Peschon J, Hartmann D, Saftig P, Blobel CP.** 2004. Distinct roles for ADAM10 and ADAM17 in ectodomain shedding of six EGFR ligands. J Cell Biol **164:**769–779. http://dx.doi.org/10.1083/jcb.200307137.
54. **Lu N, Wang L, Cao H, Liu L, Van Kaer L, Washington MK, Rosen MJ, Dube PE, Wilson KT, Ren X, Hao X, Polk DB, Yan F.** 2014. Activation of the epidermal growth factor receptor in macrophages regulates cytokine production and experimental colitis. J Immunol **192:**1013–1023. http://dx.doi.org/10.4049/jimmunol.1300133.
55. **Neufert C, Becker C, Tureci O, Waldner MJ, Backert I, Floh K, Atreya I, Leppkes M, Jefremow A, Vieth M, Schneider-Stock R, Klinger P, Greten FR, Threadgill DW, Sahin U, Neurath MF.** 2013. Tumor fibroblast-derived epiregulin promotes growth of colitis-associated neoplasms through ERK. J Clin Invest **123:**1428–1443. http://dx.doi.org/10.1172/JCI63748.
56. **Frey MR, Dise RS, Edelblum KL, Polk DB.** 2006. p38 kinase regulates epidermal growth factor receptor downregulation and cellular migration. EMBO J **25:**5683–5692. http://dx.doi.org/10.1038/sj.emboj.7601457.
57. **McElroy SJ, Frey MR, Yan F, Edelblum KL, Goettel JA, John S, Polk DB.** 2008. Tumor necrosis factor inhibits ligand-stimulated EGF receptor activation through a TNF receptor 1-dependent mechanism. Am J Physiol Gastrointest Liver Physiol **295:**G285–G293. http://dx.doi.org/10.1152/ajpgi.00425.2007.

58. **Zwang Y, Yarden Y.** 2006. p38 MAP kinase mediates stress-induced internalization of EGFR: implications for cancer chemotherapy. EMBO J **25:**4195–4206. http://dx.doi.org/10.1038/sj.emboj.7601297.
59. **Dube P, Punit S, Polk DB.** 2014. Redeeming an old foe: protective as well as pathophysiological roles for tumor necrosis factor in inflammatory bowel disease. Am J Physiol Gastrointest Liver Physiol **308:** G161–G170. http://dx.doi.org/10.1152/ajpgi.00142.2014.
60. **Roulis M, Armaka M, Manoloukos M, Apostolaki M, Kollias G.** 2011. Intestinal epithelial cells as producers but not targets of chronic TNF suffice to cause murine Crohn-like pathology. Proc Natl Acad Sci U S A **108:**5396–5401. http://dx.doi.org/10.1073/pnas.1007811108.
61. **Stadnyk AW.** 2002. Intestinal epithelial cells as a source of inflammatory cytokines and chemokines. Can J Gastroenterol **16:**241–246.
62. **Xue X, Ramakrishnan S, Anderson E, Taylor M, Zimmermann EM, Spence JR, Huang S, Greenson JK, Shah YM.** 2013. Endothelial PAS domain protein 1 activates the inflammatory response in the intestinal epithelium to promote colitis in mice. Gastroenterology **145:**831–841. http://dx.doi.org/10.1053/j.gastro.2013.07.010.
63. **Leppkes M, Roulis M, Neurath MF, Kollias G, Becker C.** 2014. Pleiotropic functions of TNF-alpha in the regulation of the intestinal epithelial response to inflammation. Int Immunol **26:**509–515. http://dx.doi.org/10.1093/intimm/dxu051.